sustainability

MDPI

Review

Stormwater Runoff Treatment Using Pervious Concrete Modified with Various Nanomaterials: A Comprehensive Review

Vahid Alimohammadi [1], Mehdi Maghfouri [2,3,*], Delaram Nourmohammadi [4], Pejman Azarsa [5,6], Rishi Gupta [5] and Mohammad Saberian [7]

[1] Department of Civil Engineering, Faculty of Engineering, Arak Branch, Azad University, Arak 3836119131, Iran; vahid.almh@gmail.com
[2] Department of Civil Engineering, Faculty of Engineering, University of Malaya, Kuala Lumpur 50603, Malaysia
[3] Hume Concrete Sdn Bhd, Wisma Hume, Petaling Jaya 46100, Malaysia
[4] School of Medicine, Shahid Beheshti University of Medical Sciences, Tehran 1985717443, Iran; dela.nourmohammadi@gmail.com
[5] Department of Civil Engineering, University of Victoria, 3800 Finnerty Rd., Victoria, BC V8P5C2, Canada; pazarsa@uvic.ca (P.A.); guptar@uvic.ca (R.G.)
[6] Kryton International Inc., 1645 E Kent Ave., Vancouver, BC V5P2S8, Canada
[7] School of Engineering, RMIT University, Melbourne, VIC 3000, Australia; mohammad.boroujeni@rmit.edu.au
* Correspondence: m.maghfouri@gmail.com

Abstract: Clean water is a vital need for all living creatures during their lifespan. However, contaminated stormwater is a major issue around the globe. A wide range of contaminants, including heavy metals, organic and inorganic impurities, has been discovered in stormwater. Some commonly utilized methods, such as biological, physical and chemical procedures, have been considered to overcome these issues. However, these current approaches result in moderate to low contaminant removal efficiencies for certain classes of contaminants. Of late, filtration and adsorption processes have become more featured in permeable concretes (PCs) for the treatment of stormwater. As nanoparticles have vast potential and unique characterizations, such as a higher surface area to cure polluted stormwater, employing them to improve permeable concretes' capabilities in stormwater treatment systems is an effective way to increase filtration and adsorption mechanisms. The present study reviews the removal rate of different stormwater contaminants such as heavy metals, organic and other pollutants using nanoparticle-improved PC. The application of different kinds of nanomaterials in PC as porous media to investigate their influences on the properties of PC, including the permeability rate, compressive strength, adsorption capacity and mix design of such concrete, was also studied. The findings of this review show that different types of nanomaterials improve the removal efficiency, compressive strength and adsorption capacity and decrease the infiltration rate of PC during the stormwater treatment process. With regard to the lack of comprehensive investigation concerning the use of nanomaterials in PC to treat polluted stormwater runoff, this study reviews 242 published articles on the removal rate of different stormwater contaminants by using PC improved with nanoparticles.

Keywords: stormwater treatment; porous concrete; nanomaterial; pollutant; permeable; adsorption

Citation: Alimohammadi, V.; Maghfouri, M.; Nourmohammadi, D.; Azarsa, P.; Gupta, R.; Saberian, M. Stormwater Runoff Treatment Using Pervious Concrete Modified with Various Nanomaterials: A Comprehensive Review. *Sustainability* **2021**, *13*, 8552. https://doi.org/10.3390/su13158552

Academic Editor: Asterios Bakolas

Received: 1 July 2021
Accepted: 28 July 2021
Published: 31 July 2021

1. Introduction

Increasing global development growth has made environmental pollution a major problem [1]. The contamination of water resources, such as seas, lakes, and rivers, is a crucial and highly considered environmental problem, since water is an important substance for life on earth, and every living creature needs freshwater to survive [2]. This is a destructive hydrological issue since it harms water quality and the ecosystem, imposing a large adverse effect on human health. Stormwater runoff accounts for the most important water contaminants. The contaminants of such a source usually include, but are not limited to, bacteria, nitrate, total nitrogen, total phosphorus and heavy metals [3–8]. Contamination from stormwater runoff is a major issue that has been enhanced by urban expansion, imposing various impervious pavement-induced problems [9,10]. This prevents passing clean runoff water from pavements into the soil, leading to inadequate replenishment of groundwater, impacting the natural water cycle. Runoff overflow is another drawback of traditional impervious pavements, which is mainly due to the pollution of streams such as fuel leakage and runoff water garbage that might degrade surface water, particularly in the form of sedimentation, flooding and erosion [11]. These downsides can be tackled by new water adsorption and filtration methods and materials [12]. A large number of eco-friendly, non-toxic and straightforward methods are currently available for the removal of contaminants, e.g., organic/inorganic contaminants and heavy metals, from stormwater based on Water-Sensitive Urban Design (WSUD), which is also known as Low-Impact Development in the United States, Sponge City in China, Nature-Based Solutions (NDS) in the EU, and Sustainable Urban Drainage Systems in the United Kingdom [13–15].

Under the umbrella of WUSD, permeable pavement (PP) allows for easy retrofitting in urban areas of large density. It significantly allows for on-site stormwater infiltration in the form of a source control measure with no urban landscape occupancy [16]. Earlier studies also suggested that PPs can be employed for the effective filtration and precipitation of the stormwater and the recharge of the groundwater resources [17]. Furthermore, PPs can decrease the implementation cost of stormwater and drainage measures [18–20]. Porous concrete (PC) can perform well when used to produce permeable pavements [21,22] since it provides environmental protection and sustainability advantages [23–25]. PC is a near-zero-slump, open-grade material containing hydraulic cement, coarse aggregates with little or no fine aggregate. It typically contains 11–35% porosity and a 7.6–51 m/h surface permeability rate. PC can readily transmit water when used as pavement or blocks [26,27]. PC, which has been widely used in Japan, USA and Europe, was developed as an environmentally friendly material in the 1980s [28,29]. The significance of using this type of material is to control stormwater runoff, restore groundwater supplies and reduce water and soil pollution. It has also been utilized in road pavements construction due to its performances of water permeation, water draining, water retention, rutting and unravelling [30]. However, this material is not suitable for the roads exposed to the heavy traffic load by vehicles.

Several mechanisms are involved in the removal of contaminants via PP. The mechanical filtration or sedimentation of pavements can trap particulate matter (PM); however, precipitation, sorption, or biologically mediated procedures can be employed to remove dissolved contaminants [31], such as organic compound biodegradation and nitrogen transformation, e.g., nitrification [32]. The filtration function of permeable concrete pavement (PCP) was extensively tested in Canada [12]. PCP was reported as the most effective material employed to remove particulate pollutants with a size of below 3 μm. Gao et al. [33] demonstrated that PCs with a void ratio of 25% and aggregate size of 10–20 mm have optimal water treatment performance. Many researchers have reported that PC is an effective material for removing suspending solids and contaminants, volume reduction in stormwater, water quality improvement, and rainfall infiltration enhancement in light of large permeability and porosity degrees. However, only a few studies were conducted on purification impacts on dissolved contaminants [34,35]. Such pollutants, including heavy metals, organic pollutants and other contaminants such as fecal coliforms (FCs) and turbidity (TU), have been removed from stormwater runoff by using PC.

The first category of pollutants consists of heavy metals, which are typically found in urban runoff. As the maintenance of water quality and sanitation infrastructures cannot compensate for large population growth and urbanization rates, the pollution of water by heavy metals is a significant issue in a large number of developing cities [16]. The sources of heavy metals may be either artificial or natural. Artificial heavy metal sources involve the direct disposal of untreated industrial waste, heavy metal contaminant-containing mining effluent, and the runoff of fertilizers and pesticides in farms. Rock outcroppings or geologic parent material is a prominent natural heavy metal source. Heavy metal contaminant composition and concentration are determined by the rock type and environmental circumstances as they activate weathering [36]. The accumulation of heavy metals may occur in the human body since they do not degrade in nature and harm human organs, including the nervous system [26,37]. To protect the ecosystem, heavy metal contaminants should be removed or decreased, while it is difficult and expensive to remove heavy metal contaminants from stormwater. To employ PCP to remove these contaminants, it is generally required to build pavements using locally available materials, resulting in a simple and economical method that does not adversely impact the environment [26]. Furthermore, Welker et al. [38] improved stormwater quality by PC infiltration and reducing common heavy metal contaminants in stormwater. Chemical metal hydroxide precipitation is probably the dominant mechanism of removing metals [39]. It is also possible to remove metal ions by the complexation and formation of calcium-attached carbonates (CO_3^{2-}) solids within concrete [40]. Fine suspending particles, however, are removed by the trapping of water and physisorption [12,41]. It was also observed that this porous medium trapped engine lubricants of simulated runoff [42]. Haselbach et al. [40] argued that experimental porous concrete maintained 90% and 87% of the Zn and Cu contents of simulated runoff, respectively. Solpuker et al. [43] studied the leakage of an aqueous solution with Pb, Zn, and Cu contents through the porous concrete. They found that Pb was fixed more satisfactorily than Cn and Zn. Greater leaching of fixed ions was observed at a pH below 8 [12,43]. PC exhibited other advantages; for instance, a PC-reactive obstruction was employed to remove the heavy metal contents of acid mine drainage by more than 75% within a column setting [23,39]. The removal of contaminants such as Pb, Zn and Cu was performed by PCP, even under cold weather—this pavement was able to retain these ions from the stormwater runoff. Therefore, the removal process of toxic heavy metals can be claimed to be independent of climatic characteristics [12,44].

The second group of contaminants is categorized into the organic pollutants category. These pollutants represent an essential source of environmental pollution and strongly threaten human health and the ecosystem [45]. As compared to heavy metals, organic contaminants have higher extensiveness and complexity [46]. Environmental organic contaminants have two major aspects, including natural and anthropogenic sources. Residual agricultural mulch, industrial dye wastewater and pesticide bottles are among the important pollutant source detection techniques [47]. Researchers developed a number of techniques for the removal of organic environmental contaminants. Such techniques include biodegradation, photolysis, hydrolysis, stripping and adsorption [48]. However, it is required to develop a wide range of techniques. The biochar adsorption of contaminants in the environment has recently been of great interest to environmental researchers [49].

PC can remove organic pollutants, such as phosphorus and nitrogen, reducing the adverse impacts of eutrophication within rivers and lakes [50,51]. A high number of studies demonstrated that PC–geopolymer combinations could remove phosphate ($PO_4{}^-P$) by 25–85%. The removal degrees depended on the contact time (0.5–8 h) within the batch reaction system [52]. A flow-through system was employed to decrease $PO_4{}^-P$ by 50% [53]. The removal of particulate matter (PM) containing total nitrogen (TN) and total phosphorus (TP) from highway pavement runoff was comparatively evaluated by Karamalegos et al. [54]. All PC types were able to remove $PO_4{}^-P$ completely in the initial $PO_4{}^-P$ concentration range of 0.06–0.85 mg/L. The significant $PO_4{}^-P$ removal of PC arises from precipitations within alkaline water [55].

The third and last category of other pollutants, including turbidity (TU) and fecal coliforms (FCs), are also important to be removed from stormwater. Water cloudiness or turbidity refers to the suspended substances (e.g., dissolved inorganics, organic compounds, organic matter, clay, and silt) of light in the water [56]. The adsorption of hydrophobic chemicals (e.g., pesticides) and heavy metals to suspended particles pose a substantial threat to health [57]. Several TU removal techniques have been developed, and a number of studies [58,59] demonstrated a 90% turbidity removal in permeable pavements. However, Pilon et al. [60] observed no considerable alternation in the removal of turbidity. As common marker organisms, total coliforms (TCs) and FCs could be employed for the quality assessment of treated water and pathogenic microorganism detection [33,61]. The presence of FCs and TCs may indicate fecal contamination. However, the literature has identified utilization limitations of traditional fecal indicators. In particular, they may be limited in their ability to indicate the overall levels of pathogens in some cases [62].

Numerous works observed PC–geopolymer mixtures to be capable of 57–100% FC removal. The rate of removal is dependent on the duration of contact (0.5–8 h) in the batch reaction system [52]. Additionally, the PC–geopolymer approach was adopted to achieve an up to 99% FC reduction [53]. A PC_{GP} pH value above 10 could lead to FC mortality. In comparison to other PC types, FC removal can be enhanced by storage layer gravel adsorption and straining as a different mechanism of removal [63]. These techniques, however, have downsides, such as often low removal rates and permeability.

It would be a novel approach to apply nanotechnology to cementitious composites for the filtration of water as it can bring a new dimension to the literature. In addition, earlier works examined a new nanomaterial and observed favorable characteristics in the adsorption-based removal of contaminants [3]. To have a considerable impact on the removal of various contaminants from runoff, the photocatalytic effect technique via nanotechnology was utilized. As a new method, photocatalysis has drawn significant attention across the world for coping with environmental pollution because it uses solar energy and thus induces no pollution. The key component of photocatalysis is a semiconductor photocatalyst [64]. A large number of photocatalytic substances have been studied, including Ag_2O, CdS, TiO_2, $SrTiO_3$, Cu_2O and MoS_2 [65]; $nTiO_2$ porous concrete (TPC) is a new effective and clean method to cope with non-point source contamination [11]. Bolt et al. [66] studied the combination of $nTiO_2$ and PC to reduce the poly-aromatic hydrocarbon (PAH) content of stormwater. The experimental findings revealed that the PC-$nTiO_2$ combination contributed to a naphthalene degradation of over 90% within four hours. This demonstrates the effectiveness of $nTiO_2$ as a remediation technique for petroleum water treatment [67]. Such a combination may be considered a candidate technique for the inorganic dye and heavy metal removal of stormwater [12].

The current paper presents an overview of the utilization of nanoparticles, as a promising material, in PC to decrease the contaminants of stormwater runoff. Several types of nanomaterials such as nano-titanium oxide (TiO_2), nano-iron oxide (Fe_2O_3), nano-Fe, nano-silica (SiO_2) and engineered Fe_2O_3 nanoparticles coated with surfactant (ENPFe-surf) are investigated to explore their impacts on the properties of porous concretes, including the permeability, compressive strength and adsorption capacity as well as the mix design of such concrete. Furthermore, the removal rate of different stormwater contaminants by using nanoparticle-improved PC was reviewed. An extensive literature search was carried out by using appropriate keywords, including nanomaterials, porous concrete, adsorption, stormwater treatment and pollutants in the databases including Scopus, Elsevier, Springer, Wiley, Taylor & Francis, etc. to retrieve the relevant articles. Ultimately, more than 220 scientific papers were found and reviewed. This comprehensive review helps the research community to navigate the existing literature and respond promptly to new challenges that arise from the rapid adoption of permeable concrete pavement technology in contaminated stormwater treatment.

2. The Impact of Polluted Stormwater Runoff and Contaminated Water on Public Health

Stormwater could be polluted with runoff gathered from rain, thunderstorms, and even melted snow due to the impervious surfaces. Such surfaces prevent stormwater from soaking into the ground, which could result in water resource contamination, especially in the urban areas—the percentage of precipitation that becomes stormwater runoff is much larger than in non-urban areas. Generally, when the stormwater flows over the land surface, it picks up numerous pollutants such as nutrients, pesticides and other chemicals from lawns and gardens, bacteria from animal and human waste, heavy metals from rooftops and cars, as well as petroleum by-products from leaking vehicles [68]. The polluted runoff can flow into the rivers and streams and may cause sewage overflows, leading to environmental effects on public health. Polluted runoff not only makes the waterways unsafe but also contaminates the drinking water sources. On the other hand, stormwater carries disease-causing bacteria and viruses [69].

2.1. Microbial Contamination

Water can be contaminated by several classes of pathogens that are excreted in feces and can cause waterborne infections, including bacteria, viruses and protozoa, which are stable in the water environment and usually are not eradicated by most of the disinfectants [70]. *Vibrio cholera* is one of the bacterial pathogens which could be found in water resources that were contaminated by feces from a person infected with cholera bacteria, which results in cholera as a diarrheal disease. This is generally the leading cause of morbidity and second most common cause of mortality among children younger than 5 years old worldwide [71,72].

Salmonella typhi is another bacterial pathogen causing typhoid fever, followed by fever, headache, constipation and skin rash as mild clinical manifestations, and some fatal diseases such as gastrointestinal hemorrhage and encephalitis [73]. This pathogen could also be spread by contaminated water [74].

Hepatitis A virus (HAV) from the picornaviridae family is a non-enveloped RNA virus that causes hepatitis A infection that does not have any prophylactic vaccine. HAV can be transmitted by the fecal–oral route, direct contact with infected individuals or contaminated drinking water by feces [75]. This virus has stability in low pH level water with moderate temperature, which results in its survival in a normal environment for months [76].

Giardia lamblia and *Cryptosporidium* are examples of pathogenic protozoa which can contaminate water resources. Giardia infection can transmit via fecal–oral route by the ingestion of the cysts [77]. Cryptosporidiosis can be transmitted via the fecal–oral route by the ingestion of oocysts present in contaminated food or water by infected human or animal feces [78]. Both of these pathogens are able to cause gastrointestinal illnesses such as diarrhea, vomiting or cramps [79].

2.2. Heavy Metal Contamination

Natural water resources contain impurities of trace elements/heavy metals. These substances, which are introduced to both surface and groundwater—through using chemicals in agriculture and the improper disposal of industrial wastes—could be dissolved by the water while moving downward as a hydrological cycle [80]. They consist of essential (e.g., Cu, Fe, Ni and Zn) and nonessential metals (Cd, Hg and Pb) [81], but many of them are toxic with a direct impact on human health, even at very low concentrations [82]. Among the heavy metals, arsenic, cadmium, lead and mercury can cause cancer, and others can only be toxic [83].

Lead (Pb) is a toxic metal that can contaminate groundwater by mine dewatering operations. This metal can be harmful to human health by ingestion or absorption of the contaminated water and have adverse effects on the central nervous system, the cardiovascular system, respiratory system, kidneys, and the immune system and also cause cancer and birth defects [84]. Iron (Fe) is generally present in groundwater resulting from the infiltration of precipitation water through underground rock formations naturally containing iron [83]. Although it is an essential element of human health conditions, excessive iron intake may have adverse gastrointestinal effects such as gastric irritation, nausea or constipation and adverse effects on growth and fetal development [85]. The presence of manganese (Mn) in water could result from natural resources such as rock and soil weathering or human activities such as mining, discharges of industries and landfill leaching [86]. Excessive exposure to manganese can cause a severe neurological disease characterized by the abnormal functioning of nerves and the loss of control over movements of the body, as well as Fe-defficiency anemia, impairing the activity of copper-dependent metalloenzymes, and some congenital disorders [87]. Cadmium (Cd), as a highly toxic heavy metal, can be released into water by the corrosion of galvanized pipes, erosion of natural deposits, metal refineries discharge and waste batteries and paint runoff. Exposure to cadmium causes acute and chronic health issues such as hypercalciuria, renal failure, kidney stones, cardiovascular diseases, anemia and lung and prostate cancer due to high exposure [88,89].

2.3. Organic Contaminants

Organic contaminants are present as pollutants in wastewater, including dye, humic substances, phenolic compounds, petroleum, surfactants, pesticides and pharmaceuticals [90], as well as pesticides, herbicides and fungicides that are abundantly used in agricultural activities, are detected in stormwater runoff [91].

The concentration of nitrate as an organic contaminant is increased in surface water and groundwater mainly due to agricultural drainage, leachate from the waste pile, fertilizers, plant humus and pollution caused by animal and human waste. The adverse effects of nitrate on humans include carcinogenesis, methaemoglobinaemia and mellitus diabetes [92,93]. The contamination of water by phosphorus can occur by point and non-point sources such as the decomposition of rocks and minerals, agricultural runoff from agricultural activities, animal wastes, sewage effluents and industrial discharges [94]. If exposed excessively, disordered mineral metabolism, calcification of the vascular system, impaired kidney function and loss of bone may occur [95]. Water may contain certain amounts of PAHs due to leaching from the soil into water or entry from industrial effluents and accidental marine spills during oil shipment. Human routes of exposure are ingestion, inhalation and dermal contact and may cause skin irritation, nausea, vomiting, diarrhea and confusion, immune function suppression, cataracts, kidney and liver damage, respiratory complications and cancer [96].

Methylene blue (MB) is an organic chloride salt, a commonly used dye—a basic dye for the coloring process, especially in the textile industry—and also can be used as antioxidant, antimicrobial, antimalarial, antidepressant, cardioprotective and neuroprotective agents. This cationic heterocyclic aromatic chemical compound with the molecular formula C16H18N3SCl is classified as a corrosive and irritant substance. The discharge of colored wastes, particularly MB dyes, which totals about 1000 tonnes/year from the textile industry, into the water resources worldwide [97], brings a serious concern in the waste treatment process as they are stable and difficult to decompose or degrade. Due to benzene, MB is considered toxic, which causes genetic mutations and negatively impacts the environment [98,99]. This chemical compound also can be harmful if swallowed and is able to cause eye irritation [100]. Industries such as textile, plastic and dye industries are sources of MB as water pollutants [101].

Copper (Cu) can enter into groundwater from metal plating, industrial and domestic waste, mining and mineral leaching [102], and may cause gastrointestinal symptoms and liver toxicity if highly exposed [103]. Some human activities such as mining, industrial usage, animal food and pesticide can release arsenic (As) into groundwater [104] and have a role in the development of liver, prostate and bladder cancer [105]. Nickel (Ni) is released by power plants, metal factories, waste incinerators and farms by its use in fertilizers [106], and its exposure is able to cause allergy, cardiovascular, kidney and lung diseases and nasal cancer [107].

The concentration of heavy metals can be measured in different regions to determine the quality of the groundwater. As an experiment, Antoneta et al. [108] measured the concentration of heavy metals as water pollutants in groundwater to identify and analyze heavy metals in the region of Tapiza, Albania. They recorded the range of heavy metals concentration in groundwater for As (2.6–9.2) mg/L, Cd (0–0.61) mg/L, Co (4.3–17.8) mg/L, Cu (7.5–28.4) mg/L, and Pb (0.96–5.84) mg/L. The heavy metals concentration value, in every region, can be compared with the standard range set by the WHO for heavy metals, such as Fe with the highest and maximum desirable limit (1.0 and 3.0) mg/L, Pb and Mn (0.4 and 0.4) mg/L, Cd (0.003 and 0.03), Cu (0.5 and 2.0), Zn (1.0 and 3.0), Hg (0.001 and

0.001) and As (0.01 and 0.01) [109]. If the resulted value is out of the given standard range, a proper water treatment would be required.

With regard to the highlighted negative effects of the pollutants in stormwater runoff and contaminated water on public health, developing a proper infrastructure such as permeable pavement by using pervious concrete could be considered as an impactful approach for efficient water management that protects, restores or mimics the natural water cycle and provides clean water.

3. Porous Concrete

3.1. Materials

As a new type of drainage base material, PC is between cement stabilized macadam and ordinary concrete, made of cement, gap-graded or single-sized coarse aggregate, water, and little volume or no fine aggregate [110]. This special concrete has little to no fine aggregate and has just enough cement paste to coat the coarse aggregate particles while preserving the interconnectivity of the voids [111]. The void ratio of pervious concrete is typically considered to be 15 to 30%—in accordance with ACI 522R-2010 [112]—depending on its application, whereas the conventional concrete is in the range of 2–4%. According to the ASTM C1688/C1688M-14a. [113], the percentage of air content (or voids) within pervious concrete is 20 $\pm$ 5% for low porosity (high compressive strength) and 30 $\pm$ 5% for high porosity (low compressive strength). Generally, high porosity leads to a high permeability for pervious concrete [114–116]. Figure 1 shows three different types of pores in PC, namely aggregate voids, air voids and pores in cement paste—these are either discrete or connected.

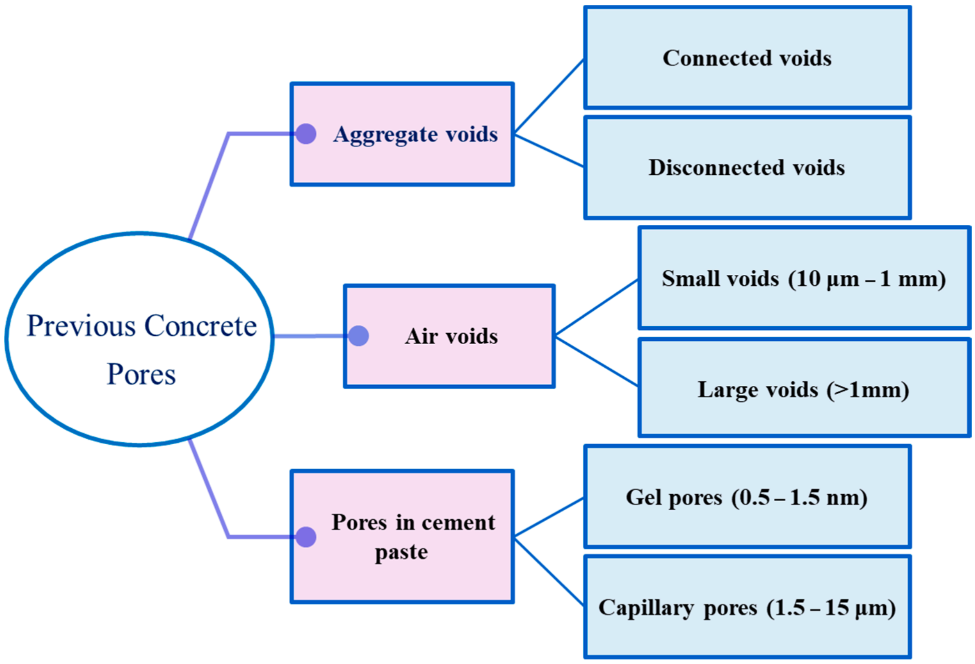

Figure 1. Different types of pores in pervious concrete [117].

Using porous concrete in pavement offers a remarkable decrease in surface runoff water by capturing and allowing rainwater to drain into the land surface [28,112]. To obtain the optimum performance of the pervious concrete pavement, its drainage rate is defined in the range of 81 to 730 L/min/m^2 [118]. This type of concrete also possesses better thermal insulation capacity, higher permeability, lower drying shrinkage and lower unit weight in comparison with conventional concrete. High porosity, however, reduces tensile, compressive and bond strengths [119,120]. The other benefits of PC roadways involve regulating stormwater, controlling contamination, separating solid substances from liquid ones and the purification of water [121–123]. Despite its numerous advantages, potential challenges, e.g., specific construction practices, a lack of standard tests, a longer curing time and specific groundwater table and expansive soil considerations, limit the use of PC [12,112].

Portland cement is a readily available binder largely employed in PCs [124]. However, it has a small strength, leading to studies that attempted to develop alternative pervious geopolymers. Nonetheless, pervious geopolymers are a relatively new topic and were investigated by a few studies. On account of a porous structure, large permeability and advantages, e.g., a water treatment ability recently found, pervious geopolymer can serve as an alternative to pervious cement concrete since it offers greater strength and higher water treatment performance [125–127]. In addition to the aggregate thickness, the aggregate size is essential and has a large impact on PCP absorption [128]. The influences of porosity characteristics on the retention of particles and a subsequent reduction in permeability were evaluated by PCPs of various aggregate sizes by Deo et al. [129]. Thus, the following subsequent sections examine PC's fine and coarse aggregates and nanoparticles.

3.1.1. Coarse and Fine Aggregates

PCs have exhibited significant performance in the harvesting and treatment of stormwater. Additionally, no pavement/curb damages have been found. Cementitious binders are major substances that trap heavy metals within the PC [130]. It is required to develop an experimental trial-grounded design to maximize the cementitious binder content while posing no impacts on void connectivity within the porous medium. It is possible to modify cementitious materials for effectively trapping toxic contaminants of industrial effluents. There is a lack of preparatory instructions to develop a PC type with controllable hydraulic conductivity in experimental settings. It is necessary to adopt an image-based approach to analyse PC pore properties, e.g., surface porosity, void size, and the volume fractions of disconnected and interconnected voids. Besides, further consideration is required for the imaging procedure of PC void connectivity [12]. Several types of coarse aggregates are employed for the production of pervious concrete, e.g., mixed river gravels, crushed limestone, cemented sedimentary and high-pressure non-foliated metamorphics [131]. However, the research cited below has shown that limestone, basalt and scoria aggregates can be used in nanomaterial-modified permeable concrete for the contaminant removal of surface water.

As a natural volcanic lightweight aggregate, scoria can be employed in place of coarse aggregates in PC [132]. As can be seen in Table 1, the dry density, bulk density, saturated density and water absorption of scoria aggregates are 1710 kg/m^3, 2150 kg/m^3, 1910 kg/m^3 and 11.90%, respectively [133]. A physical porous concrete slab model with coarse scoria aggregates was studied to understand how scoria could be employed in PC to maintain petroleum pollutants [134]. The model was utilized to calculate the water/petroleum fluid maintenance capacity of scoria, similar to those that were utilized for cleaning oil spills. A scoria leach field was employed to discharge water. The addition of scoria to PC allows for precipitation runoffs of driving surfaces to be reintroduced to local aquifers of lower contamination in order to preserve clean water [135].

Holmes et al. [136] employed coarse aggregates such as limestone gravels provided by a local hardware shop to produce PC. Limestone is a sedimentary rock containing $CaCO_3$ [137]. It was found that the calcite content of limestone powder could adsorb individual metals, e.g., Pb, Zn and Cd [136]. Table 1 shows the physical properties given above for limestone aggregates. Earlier studies sieved limestone gravels to collect aggregates with a size of 4.75–12.5 mm. In addition, the binder was composed of fly ash (FA) and Portland cement, with no fine aggregates. A fixed 4:1 aggregate/binder mass ratio was applied [23,55,138].

In another study, PC specimens were produced using basalt aggregates with a specific size of 4.75–9.5 mm, and #42.5 Portland cement [11]. Basalt aggregates had a larger fine grain content than the other types, reducing the ultimate porosity [139]. According to Table 1, the dry density, saturated density, bulk density and water absorption of basalt aggregates were 2230 kg/m^3, 2670 kg/m^3, 1500 kg/m^3 and 1.20%, respectively. Wang et al. [140] suggested that the size reduction in crushed basalt aggregates from 4–8 mm to 2–4 mm positively affected the PC's mechanical strength in light of an optimal interface.

Table 1. Physical properties of basalt, limestone and scoria aggregates.

Aggregates	Bulk Density (kg/m^3)	Dry Density (kg/m^3)	Saturated Density (kg/m^3)	Water Absorption (%)	Ref.
Scoria	2150	1710	1910	11.90	[133]
Limestone	1460, 2510	1530	2550	2.58, 1.8	[141–143]
Basalt	1500	2230	2670	1.20	[139,144,145]

Earlier studies suggested that PCPs involved several layers, including the surface layer (in porous concrete), base layer, subbase layer, coarse sand filter layer, fine sand filter layer and subgrade. PCP models have been proposed based on the AASHTO (1993) [146] guidelines and the regular layer thickness of porous concrete pavements [147]. Rahman et al. [26] applied the thicknesses of 8, 4, 4, and 8 inches to the base layer (choker coarse and filter sand layer), the surface layer (porous concrete pavement), fine sand layer (filter blanket) and sub-base layer (coarse reservoir), respectively, as shown in Figure 2. The researchers at the University of New Hampshire Stormwater Center (UNHSC) studied pavement structural layers in the pavement system. They proposed that it was necessary to place a 4–8-inch thick choker crushed stone layer (an 8-inch thick layer is preferable on account of porous asphalt compaction problems) and 8–12-inch thick sand and coarse reservoir filter layers, a filter blanket (i.e., pea gravel) with a minimum thickness of 3 inches, a perforated subdrain (Polyvinyl chloride–PVC–pipe) with a diameter of 4–6 inches below the 4–6-inch thick porous pavement layer [148].

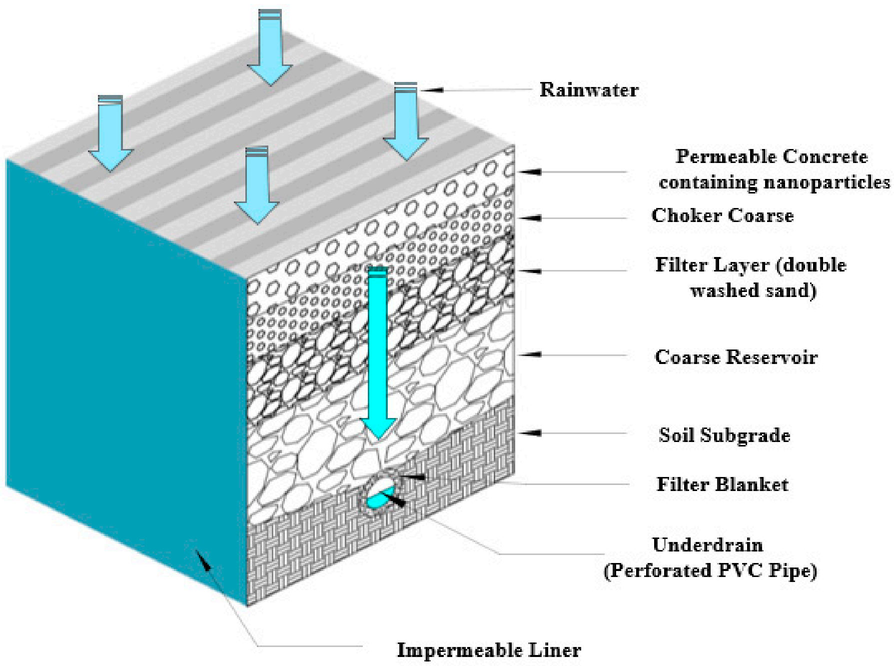

Figure 2. A schematic view of porous concrete pavement.

3.1.2. Nanoparticles Employed for the Improvement of PC and Pollutant Adsorption

In PC, nanomaterials are used as a partial replacement of cementitious material [149,150]. The use of nanotechnology for the filtration of water in cementitious composites could add a new dimension to the existing literature [12]. Generally, the inclusion of nanomaterials significantly modifies and improves fresh and hardened properties of concrete—in short-term and long-term ages—made from conventional grain-size materials [151,152]. Nano-sized materials with larger surface areas can be employed to reduce deleterious ion movement through cementitious material pores [153–155]. The literature suggests that using nanomaterials, e.g., carbon nanofibers, multiwalled carbon nanotubes (MWCNTs), TiO_2, Al_2O_3 and SiO_2 nanoparticles, to modify cementitious composites would significantly enhance the durability and mechanical properties of concretes [156–160]. It was observed that nanoparticles of larger surface areas could substantially adsorb free water, enabling greater chemical reactivity with binder phases [155]. As a result, nanomaterials are believed to be nucleation sites for early-age progressive hydration crystal growth, reducing non-hydrated cement fraction [161,162]. Moreover, superplasticizers can be added to adjust fresh concrete workability and prevent Van der Waals-induced nanoparticle agglomeration [163]. Graphene oxide (GO) is gaining popularity as an additive majorly due to its effectiveness as an adsorbent in the removal of contaminants, e.g., heavy metals, pesticides, bacteria and dyes, from aqueous solutions [164,165].

Previous studies employed SiO_2 nanopowder and Fe nano-liquid as adsorbents [24]. According to Figure 3, SiO_2 nanopowder has a mean particle size and a surface area of 20–30 nm and 180—600 m^2/g, respectively. Fe nano-solution contains 10 nm magnetite, proprietary surfactants, and water at the volumetric fractions of 2.8–3.5%, 2–4%, and 92.5–95.2%, respectively [23]. Earlier studies found the surface area of Fe nanoparticle powder varies from 14.50 to 36.50 m^2/g [166]. Previous studies utilized TiO_2 nanoparticles in the form of white powder with a particle size of 25 nm and a surface area of 50 m^2/g [11]. FA and engineered surfactant (ENPFE-surf)-coated Fe_2O_3 nanoparticles were exploited as fine additives to enhance PC's compressive strength and P removal capability [138]. The specimens with the Fe_2O_3 nanoparticle contents of 3–5% unexpectedly removed insignificant amounts of oxidation-prone contaminants, e.g., NH_4^+ and phenol. The specimen with a volume fraction of 5%, however, considerably improved the removal of Mn. Generally, despite the SA measurement of Fe_2O_3 nanoparticles at 39 m^2/g, the volume fraction did not impact the contaminant removal of the specimens containing Fe_2O_3. Therefore, they seemingly added no value to the permeable concrete [32].

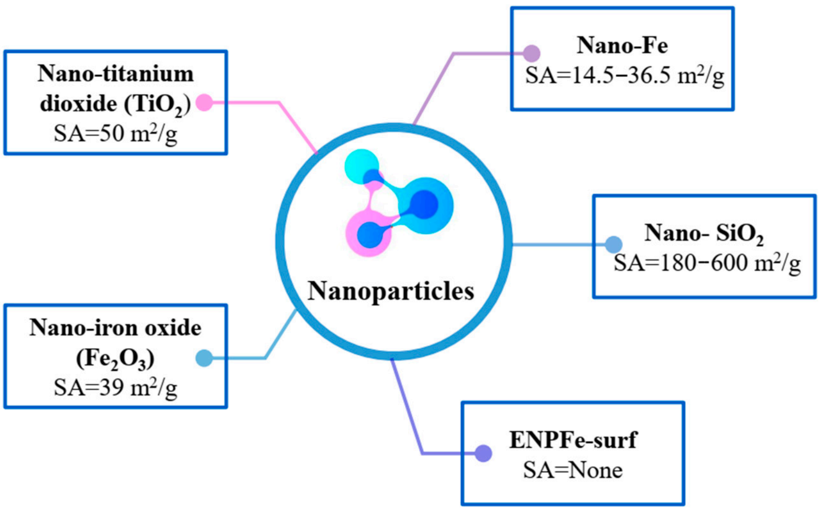

Figure 3. The investigated nanoparticles in PC.

Figure 4 represents the inter-relationships of cementitious materials, nanomaterials, coarse/fine aggregates and the water treatment process. Different nanomaterials are illustrated in Figure 3—for porous concrete production—on the grounds of their ability to adsorb contaminants. Before the mixing of concrete, potential nanomaterials are individually added to cementitious materials. Afterwards, the improved cementitious materials are mixed with fine and coarse aggregates and followed by adding the mixing water to complete the mixing process to produce modified pervious concrete. As can be seen from the treatment unit, a pipe is then applied to mould the PC to pass contaminated water for the adsorption of contaminants and treating the water.

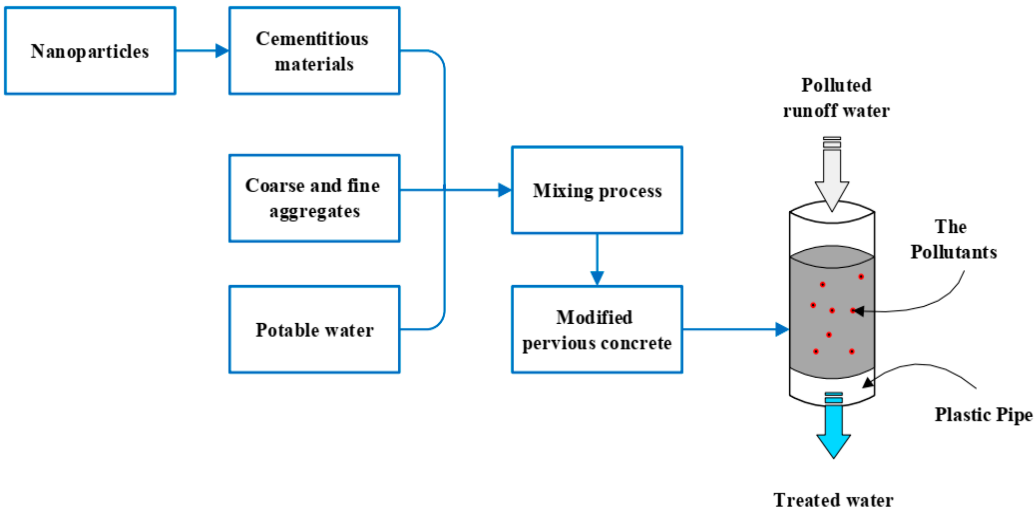

Figure 4. A schematic view of producing the improved permeable concrete and runoff water treatment procedure.

Previous studies employed aggregates with a larger number of pores. TiO_2 and SiO_2 nanoparticles were added to aggregates to fill the cracks and pores [167]. The photocatalytic layer, typically nano-sized TiO_2 nanoparticles, was recently added to permeable pavements as a new technique to reduce urban water contaminations [168]. Due to their large specific surface, TiO_2 nanoparticles enhance hydration products by filling pores and inducing nucleation. This would improve the concrete pore structure, and concrete durability properties, e.g., permeability, frost resistance and wear resistance, rise considerably [167]. It could be concluded from the obtained results that using nanomaterials would improve the PC's characteristics and remove contaminants from polluted water.

3.2. Mix Design of Nanoparticle-Improved PC

The mixture design technique of standard concrete pavements takes into account sustainability, compactability and transportability. However, it is required to incorporate further aspects in PC mixture design. It is not possible to employ conventional aggregate grading techniques grounded on the void ratio and packing density for PC. This is also the case with other standard concrete techniques since the air void system required is a challenge to the development of a standard mixture design technique. Some short and long-term properties for fresh and hardened paving concrete, such as setting time, workability and drying shrinkage, do not apply to PC. For pervious concrete, typical important properties are porosity, permeability, and compressive strength. However, flexural strength, durability against freeze–thaw cycling, impact loading, and abrasion are considered as secondary criteria for such concrete. An appropriate concrete mix design for PC will technically balance porosity/permeability and mechanical properties to meet structural and hydrological performance requirements [169].

The optimal water/binder (W/B), Fe_2O_3 NP/binder (ENP/B) and fly ash/binder (FA/B) ratios of Portland cement pervious concrete (PCPC) were determined to be 0.35, 0.05 and 0.15, respectively [138]. Coarser aggregates (larger than 4.75 mm) were subjected to narrow grading to enable rapid water percolation. This can also be performed by reducing the fine aggregate content. Table 2 provides the most commonly used coarse aggregate grading of PC mixes based on ASTM C33 [170].

Table 2. Most common PC aggregate grading [156].

Size Number (Nominal Size)	Amounts Finer than Each Laboratory Sieve, Mass Percent							
	25 mm	19.0 mm	12.50 mm	9.50 mm	4.75 mm	2.36 mm	1.18 mm	300 μm
#67 (19.0 to 4.75 mm)	100	90–100	-	20–55	0–10	0–5	-	-
#7 (12.5 to 4.75 mm)	-	100	90–100	40–70	0–15	0–5	-	-
#8 (9.5 to 2.36 mm)	-	-	100	85–100	10–30	0–10	0–5	-
#89 (9.5 to 1.18 mm)	-	-	100	90–100	20–55	5–30	0–10	0–5

The coarse aggregates had a size of 4.75–25 mm, while the fine aggregates had a size of 0.3–4.75 mm. Table 3 represents common ratios in PC mixes. As can be seen, the porosity degree was 15–35% based on ACI 522R-2010 [112].

Table 3. Typical proportions of material in porous concrete [101].

Details	Proportions in kg/m^3
Cementitious materials	270 to 415
Aggregate	1190 to 1480
w/c ratio, by mass	0.27 to 0.34
Aggregate: cement, by mass	4 to 4.50:1
Fine: coarse aggregate, by mass	0 to 1:1

At a porosity degree below 15%, concrete pores are argued to be of insignificant interconnectivity, disrupting rapid water percolation [171]. nTiO_2 aqueous dispersions of 0.5, 1.0 and 1.5 g/L and the nTiO_2 addition techniques of painting, soaking and dipping were employed to evaluate the purification potential of TiO_2-improved PC for contaminated runoffs. Painting is the diversion of 200 mL nTiO_2 aqueous dispersions on the surface of the specimen using a brush, soaking refers to the soaking of concrete within a 200 mL solution, and dipping applies a pipette to divert 200 mL nTiO_2 aqueous dispersions to surface pores. Next, the specimens are kept in the water for thirty minutes until no white liquid precipitates exist. Nine different concrete mixtures were prepared with a total of twenty-seven specimens (three specimens per concrete mixture) to repeat the tests for higher accuracy. Table 4 represents the nTiO_2 treatment and mix design of the PC specimens.

Table 4. Mix design and nTiO_2 treatment of the PC specimens [11].

Sample Number	nTiO_2 Application Methods	TiO_2 Solution (g/L)	W/C	Material Contents (%)		
				Cement	Water	Aggregate
1	Dipping	0.50	0.31	15.80	4.90	69.30
2		1.00				
3		1.50				
4	Painting	0.50				
5		1.00				
6		1.50				
7	Soaking	0.50				
8		1.00				
9		1.50				

Previous studies employed type I Portland cement grounded on ASTM C150-07 (2007) [172]. The coarse aggregates had a size of 10–12.5 mm according to the ASTM E 647 [173], whereas the fine aggregates had a size of 4.75–9.5 mm according to ASTM E. 01 [174]. The water/cement and coarse aggregate/cement ratios were 0.4 and 3.64, respectively [32].

PC generally requires more comprehensive quality control protocols during mixture proportioning in comparison with normal PC. This is mainly because the content of paste and nanomaterial is particularly critical to ensure that they are fully blended and adhered to the aggregates. The moisture level of aggregate and its size should also be monitored, since the absorbed water by the aggregates in PC allows the porosities to be well connected with appropriate strength and satisfactory permeability.

3.3. Permeability, Compressive Strength, Adsorption Capacity and Regeneration Process of PC

PC permeability is often measured by the falling head test principle. Porous permeability is determined by the pore count and connectivity, while porosity refers to volumetric material property [175–177]. The Kozeny–Carman formula [114] defines the relationship between porosity and permeability of a porous material as:

$$K = \left(N^3\right)/(F \times \tau^2 \times S^2 \times (1-N)^2) \quad (1)$$

where N denotes porosity, τ represents the tortuosity (i.e., the opposite of connectivity), F accounts for different pore shapes, and S incorporates the specific pore surface area. Low- and high-paste PCs were fabricated and subjected to experimental evaluation to examine permeability. Sumanasooriya et al. [178,179] suggested that a rise in the binder content diminished PC porosity based on paste clogging localization. This could raise flow channel tortuosity, decreasing the permeability of water. Additionally, a large paste content diminished the pore structural connectedness of the concrete system. Higher PC paste contents, higher compaction effort and fine aggregates and grading may yield small permeability due to decreased permeable pores [128,180,181]. The coefficient of PC permeability (i.e., hydraulic conductivity) is typically obtained to be 1.4–12.3 mm/s. Large porosity, however, diminishes PC strength, typically yielding a compressive strength of 3.5–28 MPa [182,183]. The permeability of the porous mixtures was found to be 1–2 cm/s. This permeability value is recommended in pavement drainage layers [184]. It was also suggested that permeability could be calculated as

$$\text{Permeability} = (4 \times V_w \times L)/\left(\pi \times D^2 \times \Delta h \times t\right) \quad (2)$$

where V_w denotes the collected volume of water at a time t, Δh represents the fixed water head, D is the PC specimen diameter, and L is the PC specimen height [23]. López-Carrasquillo and Hwang [23] reported the permeability and compressive strength of a PC with a fly ash content of 24% and a $nSiO_2$ content of 1.9% to be 8.8 mm/s and 17.3 MPa, respectively. Besides, a high fly ash content (i.e., 60%) led to lower abrasion resistance and compressive strength. Jo et al. [52] studied a PC with the fly ash and SiO_2 contents of 60% and 0.04%, respectively. They found the compressive strength and permeability to be 5.0 MPa and 4.3 mm/s at the age of seven days, respectively. Soto-Pérez et al. [55] applied a fly ash content of 35% and a Fe_2O_3 nanoparticle content of 6%. They calculated the compressive strength and permeability to be 22.8 MPa and 5.6 mm/s at the age of twenty-eight days, respectively [32]. Furthermore, the porosity and permeability of the basalt-aggregated PC were reported to be 20% and 15 cm/s, respectively [11]. In general, nanoparticles that substitute cement decrease permeability since nanoparticles have a larger specific surface area than cement. As a result, the absorption of free water in the concrete mix is enhanced. SiO_2 nanoparticles in concrete yield a smart material with fewer microcracks and a larger density than regular concrete. Concrete obtains water resistance as microcracks reduce [185].

Table 5 shows the mean compressive strengths of the specimens at a curing age of 28 days. As can be seen, all the modified permeable specimens had larger compressive strengths than the control specimens. The SiO_2-containing specimens exhibited the largest compressive strength rise. The PCs containing Fe, Fe_2O_3, ENPFe-surf, and TiO_2 nanoparticles were found in the next ranks, respectively. The maximum permeability rate of the specimens was evaluated, which could largely vary depending on the nanoparticles. All nanomaterials containing PC showed a lower permeability than the control mixes, except for ENPFe-surf. One can say that enhanced compressive strength leads to the reduction in permeability.

Table 5. Effect of various nanomaterials on the mechanical properties of PC.

Nanoparticle	Dose	Permeability (CM) + (mm/s)	MCS ++ (CM) + (MPa)	Ref.
TiO_2	0.5–1.5 (g/L)	1.99–2.19 (2.21)	18.65–22.04 (18.16)	[11]
Fe_2O_3	3 and 5%	−(8.39)	−(6)	[32]
Fe_2O_3	6% (NI/B *) 0.5% (NI/B)	5.60 (26.70) 7.60 (26.70)	22.80 (13.90) 21.40 (13.90)	[55]
Fe SiO_2	30 (kg/m^3) (6.30%) 2.28 (kg/m^3) (0.50%)	9.40 (15) 8.80 (15)	16.20 (9.60) 17.20 (9.60)	[23]
ENPFe-surf	5% (ENP/B)	18.80 (11.5)	10.41 (7.93)	[186]

* Fe_2O_3 nanoparticle-to-binder, + control mix, ++ modified compressive strength.

Porous pavements are usually regarded as being successful in removing pollutants by adsorption [187,188]. The ettringite significance of heavy metal adsorption is an essential contributor to PC ability, as this heavy metal adsorption mechanism does not involve heavy metal detachment, particularly for soil adsorption [189]. Thus, it applies in situ infiltration to avoid underground water contamination [190]. Concerning the removal of heavy metals, adsorption is considered the main mechanism of interaction for geopolymer concrete. It should be mentioned that experimental tests on adsorption were mostly performed at a laboratory scale to remove a single heavy metal of synthesized polluted solutions. However, a multi-complex setting is the challenge of heavy metal contaminants in real-life conditions [3]. Kara et al. [191] employed real-life contaminated water to evaluate the impacts of Metakaolin (MK)-based conventional geopolymer on the removal of Co^{2+} and Mn^{2+} ions. The removal efficiency of conventional geopolymer was observed to be 2–3 times lower for real-life contaminated water than the synthesized scenario, which might have resulted from a competition with heavy metal ions and other cationic species to bind onto the geopolymer surface. Ge et al. [192] and Kara et al. [193] carried out column and batch adsorption investigations to remove heavy metals through a geopolymer. The column test was aimed to simulate the real-life processes of industrial adsorption. The batch adsorption test might fail to suit PC since PC is often employed in pavements. Water typically infiltrates through the matrix instead of temporarily remaining in the medium, which is the case in batch adsorption. As a result, column or dynamic adsorption is preferable for the study of removal impacts [194].

PC consists of paste-wrapped aggregates [195]. Stormwater engages in a contact majorly with the inner pore walls when it infiltrates through PC pores. Sansalone et al. [196] demonstrated that PC's capacity to absorb heavy metals and harmful stormwater substances majorly arise from the paste layer resting on the inner pore walls. The paste adsorption capacity of PC is known to strongly impact its capacity to purify water. Moreover, further insights suggest that the runoff water–paste contact area and time also impact water purification performance. The runoff water–paste contact area and time are known to be dependent on the paste/aggregate (P/A) mass ratio and the bulk porosity of aggregates (BPA). The paste absorption capacity, BPA, and P/A ratio primarily determine the PC's capacity to purify water [197]. For a constant adsorption capacity of the paste, an alternation in BPA and P/A ratio may directly impact the PC adsorption capacity, influencing its capacity to purify water. Today, the study of volumetric structural impacts on the PC's capacity to purify water is majorly focused on the BPA impacts. Previous investigations reported that a rise in BPA increased PC's capacity to adsorb contaminants, e.g., heavy metal ions, significantly improving the capacity to purify water [198,199]. However, some other researchers proposed that a reduction in the BPA adds to stormwater passage time, allowing for the improvement of the contaminant removal rate and obtaining greater water purification performance [51,200]. In summary, the two volumetric structural parameters, including the BPA and P/A ratio, simultaneously impact the PC's mechanical properties, water permeability and water purification. Hence, in order to develop a PC to purify water, it is required to shed light on the BPA and P/A impacts on mechanical properties, water permeability, water purification, and their relationships [197].

Figure 5 represents the increment percentage of compressive strength and decreasing percentage of the permeability due to the inclusion of nanoparticles. It can be observed that the addition of 5% ENPFe-surf leads to an increase in the permeability up to 63%, as opposed to adding other nanoparticles, including TiO_2, Fe_2O_3, Fe and SiO_2, which decrease the permeability up to 10%, 79%, 37% and 41%, respectively. However, the addition of the nanoparticles considerably increases the compressive strength by 21%, 64%, 69%, 79% and 31% when using TiO_2, Fe_2O_3, Fe, SiO_2 and ENPFe-surf nanoparticles, respectively.

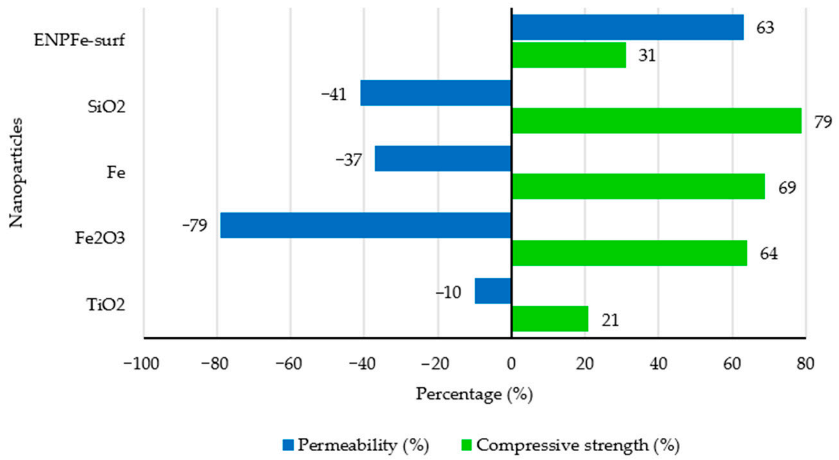

Figure 5. Variations of compressive strength and permeability (in %) due to the addition of nanoparticles [11].

The clogging factor due to the contaminant of stormwater with dirt and debris in the adsorption process can be considered as an operational issue, which may result in decreasing the performance of the treatment unit and finally leading to the failure of the system. Therefore, the longevity of the stormwater treatment system is an important parameter for acceptable performance [201]. Appropriate maintenance and regeneration methods should be implemented to enhance the long-time serviceability of porous pavement for an adequate adsorption capacity and infiltration rate. The most widely used mechanical and manual rehabilitation techniques to prevent the permeable pavements from saturating and clogging are pressure washing, sweeping with a broom, vacuum cleaning and the combination of both vacuum sweeping and pressure washing [202]. Previous researchers reported that the regeneration of porous concrete blocks could be performed using brooming and pressure washing [203]. In vacuum sweeping, as another proposed regeneration method, the debris is sucked out from the voids to re-open the clogged pores. While vacuum sweeping is reported as one of the fastest methods, it is not as effective as pressuring washing [202]. The American Concrete Institute (ACI) suggested that one of the most effective regeneration methods is combining the power vacuum after pressure washing [204]. Chopra et al. [205] also claimed that the combination of the pressure washing and vacuum sweeping showed the highest recovery rate in permeability in comparison with only the pressure washing technique, which was not so effective. While earlier studies on clogging confirmed that the rejuvenation and maintenance methods were more effective and easy on the pervious pavements with high porosity percentages, pavements with porosity lesser than 15% had a trivial outcome in the regeneration process [206,207]. Consequently, it should be noted that the retrieval rate is mainly influenced by the pore connectivity, pore size distribution and porosity of previous pavements [202].

4. The Investigated Stormwater Contaminants

Today, contaminants are increasingly introduced into water supplies due to human activity-related substances, resulting in the emergence of serious concerns around the world. Traditional toxic contaminants such as oxyanions and heavy metal cations are recognized to strongly threaten the ecosystem and human health [208]. Nowadays, porous pavements improved with nanomaterial are being employed to remove a wide range of contaminants, e.g., iron (Fe), manganese (Mn), lead (Pb), nitrate (NO_3), orthophosphate as phosphorus (PO_4^-p), phosphorous (P), phenol (Ph), ammonium (NH_4), ammonia nitrogen (AN), total phosphorus (TP), methylene blue (MB), poly-aromatic hydrocarbon (PAH), turbidity (TU) and fecal coliforms (FCs). As shown in Figure 6, the authors of this study have categorized the pollutants into three categories: (1) heavy metal pollutants, (2) organic pollutants, and (3) minor pollutants such as TU and FCs (other pollutants). Surface water resources, specifically natural rivers, receive all three types of pollutants from industrial and municipal wastewater sources, non-point source contaminants, and organic chemicals [209].

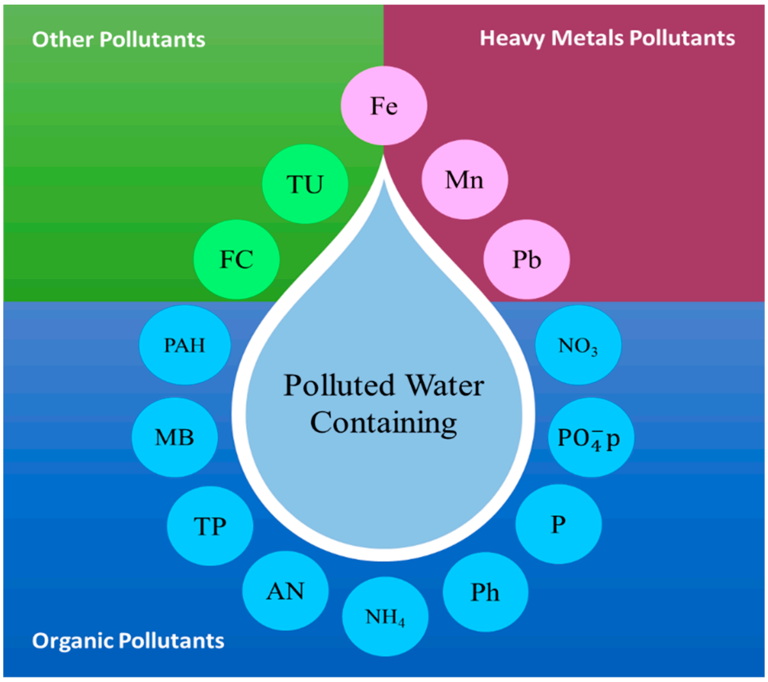

Figure 6. The investigated stormwater contaminants in this study.

Among source-traceable contaminants, heavy metal pollutants are the first category of water contaminants that are high risk with the ability to impose threats to human health and the environment [210]. They are inorganic elements with a density above 5 g/cm^3 [210]. Heavy metals are typically harmful and have great toxicity, even at small concentrations. These pollutants have several adverse effects on human health and the environment [211]. For instance, long and strong Cu exposure might result in kidney damage, and Pb poisoning also causes the failure of the kidney. Such effects arise from non-biodegradability, great toxicity and bioaccumulation in food chains and living organisms [212].

Researchers suggested that remediation and management efforts should be developed to protect human health in areas facing contaminated water containing heavy metals [213]. Apart from the heavy metals, organic contaminants as the second category are capable of inducing serious hydrological issues. These contaminants typically arise from runoff, industrial wastewater and domestic sewage penetration. At an excessively high concentration of nutrients (e.g., N and P) in the water, the quality of water is impacted by eutrophication [214]. Eutrophication depletes dissolved oxygen and enhances toxic cyanobacteria growth [123]. Harker and Mahar [134] evaluated the release of nutrients into waterways by untreated stormwater discharge. Petroleum products and fertilizer-induced nitrates contaminate local waterways and groundwater resources [135].

Methylene blue is a standard adsorbate used as a representative printing agent. Additionally, the eutrophication of water is considered to arise from nutrient contaminants, TP, and ammonia nitrogen ($NH_3{}^{-}N$) as the major elements. Consequently, algae and other planktons quickly propagate and reduce the dissolved oxygen content and water quality, leading to the enormous death rates of fish and other organisms. Hence, it is crucial to hinder and control organic pollutants such as NH_3N and TP to protect the aquatic ecosystem [11]. In this regard, the removal of these pollutants by geopolymer has been reported by previous research.

Other pollutants, including FC and TU, are discussed as the third category of contaminates in this study. Fecal coliform, as a fecal indicator bacterium, is typically performed to evaluate the microbial quality of surface waters, such as stormwater runoff. Since contamination in surface water by pathogens is a major concern around the world, such indicator bacteria determine the presence of fecal matter and, therefore, the possible existence of pathogens [215]. Facing pathogenic bacteria from recreational contact with surface water resources may lead to health issues, such as nose and eye infections, skin rashes and acute gastrointestinal illness, including diarrhea and cramps [216]. To date, there the concept of removing FC pollutants from surface water has drawn significant attention [217].

Water turbidity or water cloudiness results from suspended particles in water due to the scattering of light [218]. Turbidity is generally considered as one of the most common parameters for the measurement of water quality [219]. Increasing turbidity causes an increase in the inactivation rates. This prevents solar power densities and moderate temperature from being reached, which may lead to the facilitation of bacterial regrowth. The ability to inactivate or kill bacteria is largely dependent on the water quality (turbidity). Therefore, to enhance the maximum bacterial inactivation, the turbidity water should be decreased [220].

5. Effect of Nanoparticles on the Removal Percentage of Contaminants

5.1. The Process of Removing Pollutants Using PC

The common aggregate-independent removal mechanisms within hydrated cement matrixes include adsorption, absorption, internal metal diffusion and co-precipitation. The mechanisms of treatment comprise chemical sorption and physical filtration [59]. Molecule accumulation on the adsorbent surface is known as adsorption. An adsorbent is a substance adsorbing molecule, while substances that are absorbed by the adsorbent are referred to as adsorbates. Basically, adsorption arises from the unbalanced adsorbent and absorbate surface molecule forces. It is typically described via isotherms; that is, the adsorbate content of an adsorbent is determined by the gas pressure/liquid concentration of the adsorbent at a fixed temperature. Researchers introduced fifteen isotherm models [221]. However, those of Langmuir [222] and Freundlich [223] are more frequently employed. One can represent a general adsorption isotherm as:

$$S = \frac{K_s C^{\beta}}{1 + \eta C^{\beta}} \tag{3}$$

In which K_s is the adsorption isotherm coefficient (in $M^{-1}L^3$), s is the adsorbed mass (in M), and C denotes the adsorbate concentration (in $M\,L^{-1}$). The equation changes into the Langmuir Equation at $\beta = 1$, into the Freundlich Equation at $\eta = 0$, and into a linear adsorption isotherm at $\beta = 1$ and $\eta = 0$. Based on the methodology of [224], the concrete blocks undergo jaw crushing and sieving with a 2 mm mesh opening.

Figure 7 depicts an SEM cement-coated aggregate image. The average metal transport and ultimate locations can be found inside the concrete. According to Figure 7, a cement-coated aggregate piece with a width of nearly 1 mm exits in the bulk material. Generally, Pb, Cd, and Zn are of proper distribution, excluding the central feature, labeled A in the backscattered section. The highlighted or white sections represent larger Zn and Cd concentrations, while Pb has higher diffusion. The feature, labeled A, stands for a crack in the concrete forming before the jar test. Figure 7 provides a detailed representation of the crack. In the vicinity of the surface aperture, larger Pb, Cd, and Zn concentrations exist. The reduction in the concentration to that of the buck metal 25–50 µm from the crack center induces a mild diffusion gradient.

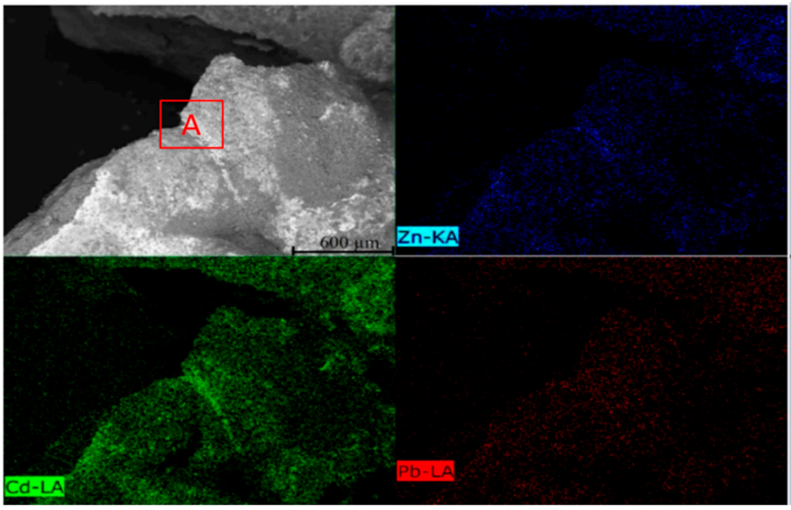

Figure 7. Cement cracks standing for precipitates and diffusion [136].

It is most probable that the cracks are formed due to demoulding or chemical shrinkage and propagate from the surface towards the inner parts of the cement hydration products. Concrete cracks may somewhat represent autogenous healing at water exposure. The permeation of water into the crack to meet the unhydrated cement grains that have newly been exposed begins secondary cement hydration. The crack could be filled with new hydration products in secondary cement hydration [225]. Secondary hydration undergoes the same stepwise process as that of primary hydration, and Ca ions also dissolve into the solution. Under heavy metal-containing solution exposure, the chemistry and morphology of cracks become a desirable deposition candidate, which was observed for Cd earlier. Pb also had the same process but to a significantly lower degree. A reduction in the Cd and Zn concentrations from the crack center to the bulk paste somewhat demonstrates diffusion [136].

In comparison to the monolithic concrete layer, the concrete fragments undergo a specific surface area enhancement after crushing. Thus, the chemical processes accelerates within the water–concrete mixture. Crushed concrete filters are proposed to remove dissolved chemicals (such as heavy metals and P) from stormwater pond effluents through interception, sorption, and filtration [226]. Particles of larger sizes are trapped at the top of the pavement in the beginning. Then, the runoff flow pushes the particles of smaller sizes throughout the layer [227].

5.2. How Adding Nanomaterials Can Enhance PC (Structure, Stability, Morphology)

The significant potential of nanotechnology should be unlocked for PCP environmental advantage maximization. For example, one can better characterize and model the underlining microscopic processes and interactions to significantly enhance insights into the contamination removal of PCPs. In binder hydration, nano-modification can alter PCPs for inducing physicochemical characteristics favouring the removal of contaminants, reduction in noise, and mitigation of the heat island effect. The application of nanotechnology to PCPs is expected to allow for an extended utilization of water and industrial by-products with no threats to environmental performance, durability, or engineering properties [21].

With the use of TiO_2 and SiO_2nanoparticles, the aggregates are loaded with these nanoparticles, which fill the cracks and pores of the aggregates. Furthermore, the specific surface area of TiO_2 nanoparticles is larger than 500 cm^2/g in general, which is highly reactive. Pore filling and nucleation raise hydration products, helping aggregates to enhance load photocatalysts. Additionally, nanoparticle filling and nucleation result in concrete structure improvement, allowing for a significant improvement of concrete durability properties, including frost resistance, impermeability and wear resistance [167]. Commercially available silicon-coated TiO_2 nanoparticles were employed in a previous study. It was found that the nanoparticles served as both a physical envelope and a chemical bond. $Si(OH)_4$ served as a strong electron directly attached to and activated the surface hydroxide Ti-OH group of the TiO_2 nanoparticles. This group converted into a Ti-O-Si bond and broadened the light absorption wavelength range of the TiO_2 nanoparticles. Then, it increased the ultraviolent absorption capacity and improved the significant degradation effect [228].

Pacheco-Torgal and et al. [229] reported that nanoparticles enable a substantial rise in the strength of cementitious composites. Such particles could fill the calcium–silicate–hydrate (C-S-H) structural voids and yield a cement binder of larger density and hardness. Heikal and et al. [230] found that SiO_2-containing composite cement optimized the mechanical properties. Theoretically, fewer voids yielded greater strength within hardened cement. This indirectly enhanced the strength of the porous concrete pavement and hardened cement binder [231]. The addition of SiO_2 nanoparticles to cementitious materials was reported to be helpful in the chemical decomposition control of HCS- Ca_2O_4Si hydrate in the water penetration of Ca. This could be attributed to the significant pozzolanic activity of SiO_2 nanoparticles, concrete pore filling, C-S-H gel formation, and small pore removal in the structure of the silicate gel, leading to a lower penetration of water and the greater durability of concrete [185].

Furthermore, SiO_2 nanoparticles are capable of serving as a nanofiller for filling up the space between the C-S-H gel particles. Additionally, nano-silica is pozzolanic and has a large pozzolanic reaction rate, as it has a high ratio of the surface area to the volume, allowing for significant chemical activity. The pozzolanic reaction of SiO_2 nanoparticles and CaOH raises the C-S-H content, enhancing the durability and strength [151,232]. All results indicated that nanomaterials enable to the improvement of the reinforcement mechanisms of PC from the perspectives of binder–aggregate interfaces and the chemistry of binder materials. Indeed, during the process of binder hydration, the PC properties can be altered by nanomaterials to induce the desirable formation of physicochemical characteristics for pollutant removal.

5.3. Impact of Nanomaterials on the Improvement of the Pollutants Removal

Metal NPs and nanocomposites, particularly silver nanoparticles (AgNPs), have recently been of interest in light of unique chemical and physical properties from large surface areas and small sizes. AgPNs can potentially be employed for the removal of metals [233,234]. However, it is difficult to apply such adsorbents in continuous flow systems because of instability and small size. To tackle this drawback, AgNPs were utilized in combination with other sorbents, e.g., carbon nanotubes and porous concrete pebbles [235,236].

According to Table 6, Fe_2O_3-improved PC can be employed for the removal of Pb, Fe and Mn by 76.80–78.40%, 84–87.7% and 46–58.70%, respectively. TiO_2 nanoparticles imposed greater degradation on account of a larger pore area and a greater number of pores for a pore size of below 10 nm. This indicates that the nanoparticles altered the cement paste microstructure [237]. Previous studies found that TiO_2 powder enabled the NO_3 removal of an aqueous solution through photocatalytic reduction [238]. Three TiO_2 powder specimens were studied at a 1 g/L concentration within a UV-irradiated solution to make the photocatalytic activity easier. It was observed that the powder specimens reduced NO_3 within an unlit setting in one hour [238]. Dylla et al. [239] observed the NO_3 removal of

TiO_2-coated concrete; however, TiO_2 exhibited a capacity of maintaining NO_3 [237]. It could also serve in removing up to 90% of methylene blue, ammonia nitrogen and TP, as well as removing P as common stormwater contaminants [55]. Previous experiments have shown PC can properly decrease TP, TN and dissolved phosphorus [51,122,123]. Hence, a pervious geopolymer has the potential to remove such contaminants. Jo et al. [52] employed a pervious geopolymer and removed P contents of treated wastewater effluent. The P removal of a pervious geopolymer may be concluded to arise from amorphous calcium phosphate ($Ca_3(PO_4)_2$) and/or hydroxyapatite ($Ca_{10}(PO_4)_6(OH)_2$), in which Ca^{2+} ions leach from the pervious geopolymer concrete [240,241]. Other mechanisms, e.g., PO_4^-p adsorption onto PCs and/or storage gravels, are believed to be possibly involved in the reduction of PO_4^-p [23]. While Fe_2O_3-improved PC nanomaterial cannot adsorb phenol and NH_4 pollutants [11], Fe_2O_3-improved PC can be employed for the removal of P by 40.50–49.80%. According to Table 6, Fe and SiO_2 nanoparticles have the potential to remove PO_4^-p by above 80%. The use of engineered Fe_2O_3 nanoparticles coated with surfactant (ENPFe-surf) enhanced P's removal in pervious concretes compared to those without ENPFe-surf coated concretes.

Table 6. Effect of various nanomaterials on the pollutants removal.

Nanoparticle	Dose	Contaminant	Removal Rate (%)	Ref.
TiO_2	1 (g)	NO_3	100%	[237]
TiO_2	0.5–1.5 (g/L)	MB	60–90	[11]
		TP	60–90	
		AN	60–90	
Fe_2O_3	3%	Fe	84	[32]
	5%	Fe	87.7	
	3%	Mn	46	
	5%	Mn	58.79	
	3%	Pb	76.8	
	5%	Pb	78.4	
	-	$NH^-{}_3N$	NE *	
	-	Phenol	NE	
Fe_2O_3	6% (NI/B **)	FC	72.4	[55]
	6% (NI/B)	P	49.8	
	0.5% (NI/B)	FC	77.9	
	0.5% (NI/B)	P	40.5	
Fe	30 (kg/m^3) (6.30%)	Turbidity	NE	[23]
		PO_4^-p	>80%	
		FC	>80%	
SiO_2	2.28 (kg/m^3) (0.50%)	Turbidity	NI ***	
		PO_4^-p	>80%	
		FC	>80%	
ENPFe-surf	5% (ENP/B)	Phosphate	Increased (7%)	[186]

* No effects, ** Fe_2O_3 nanoparticle-to-binder, *** Negative impact.

Previous studies have shown PC can properly decrease FC [55]. An FC removal of above 95% was performed by adding SiO_2 nanoparticles to PC (PC_{NS}) and a control PC (PC_{CT}). An FC removal of below 80% for both PC containing Fe nanoparticles (PC_{NI}) and Portland cement GP (PC_{GP}), and an FC removal of below 40% for PC_{NI} in the second phase can be considered to stem from an unusually large initial FC concentration of 3×10^4 CFU/100 mL [242]. $Fe_2O_3{}^-$ improved PC can also be employed for the removal of FC by 72.40–77.90% [55]. Furthermore, Fe and SiO_2 nanoparticles were able to remove FC by over 80%. Whereas Fe nanoparticles were not found to be involved in turbidity removal, SiO_2 nanoparticles posed a negative effect on turbidity treatment.

It is noteworthy to mention that the performance of pollutants removal with the use of various nanoparticles in PC is significantly different. Figure 8 indicates that PC containing

TiO_2 nanoparticles enables the removal of NO_3, MB and TP by almost 100%, 30% and 30%. For example, PC made with Fe_2O_3 nanoparticles can remove more pollutants compared with ENPFe-surf, Fe and SiO_2 nanoparticles. While increasing the percentage amount of Fe_2O_3 nanoparticles from 0.50% to 6% results in the reduction in FC and P removal by 5.50% and 9.40%, respectively, the removal percentages of Fe, Mn and Pb decrease up to 37.70%, 12.79% and 1.60%, respectively. Furthermore, for the addition of 0.50% SiO_2 and 6.30% Fe nanoparticles, the difference between the removal percentage of PO_4^-p and FC is completely similar, accounting for more than 80%. Similarly, the percentage of phosphate removal experiences an increasing trend to 7% when adding ENPFe-surf to PC. It should be noted that the zero values mean that the removal process was been investigated or the nanoparticles did not affect the pollutants' removal.

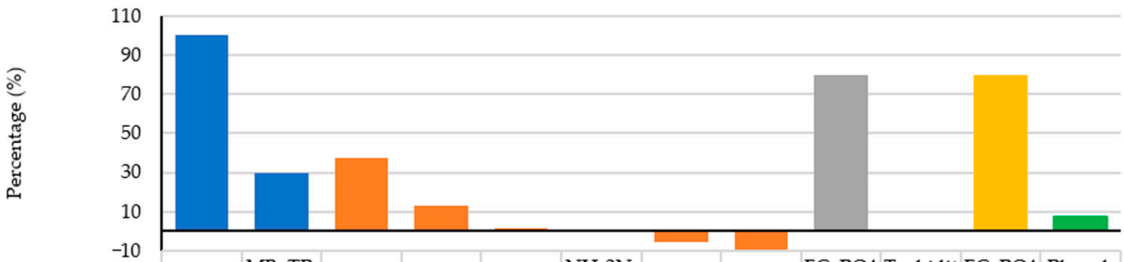

	NO3	MB, TP, AN	Fe	Mn	Pb	NH-3N, Phenol	FC	P	FC, PO4 p	Turbidity	FC, PO4 p	Phosphate
TiO2	100	30	0	0	0	0	0	0	0	0	0	0
Fe2O3	0	0	37.7	12.79	1.6	0	−5.5	−9.4	0	0	0	0
Fe	0	0	0	0	0	0	0	0	80	0	0	0
SiO2	0	0	0	0	0	0	0	0	0	0	80	0
ENPFe-surf	0	0	0	0	0	0	0	0	0	0	0	7

Figure 8. Percentage removal changes of pollutants using different nanoparticles [237].

6. Conclusions

According to a survey of the literature, nanoparticles can be used to develop a high-performance PC for specific applications. This is due to the fact that nanomaterials increase a variety of technical qualities in cement-based materials. In this context, the current study looked into the features of nanoparticle-modified PC for removing pollutants from runoff and stormwater. Nano-titanium oxide (TiO_2), nano-iron oxide (Fe_2O_3), nano-Fe, nano-silica (SiO_2), and engineered Fe_2O_3 nanoparticles coated with surfactant (ENPFe-surf) are among the nanomaterials reviewed in this study in the development of the nano-based permeable lightweight concretes. For this purpose, 242 scientific published papers were reviewed in detail. The most important results are as follows:

1. All PC specimens improved with Fe and SiO_2 nanoparticles were found to have satisfactory performance in removing FC and PO_4^-p. However, while PC improved with Fe nanoparticles did not affect the turbidity (TU) removal, the PC modified with $nSiO_2$ negatively affected the removal of TU.
2. The addition of TiO_2 nanoparticles to PC (i.e., TPC) imposed greater degradation on account of a larger pore area and a greater number of pores for a pore size of below 10 nm. This indicated that the nanoparticles altered the cement paste microstructure, resulting in the improvement of the removal of the organic contaminants, including ammonia nitrogen (AN), total phosphorus (TP), nitrate (NO_3) and methylene blue (MB).
3. The mean removal rates of heavy metals (Fe, Mn and Pb) significantly improved using PC specimens with Fe_2O_3 nanoparticles, but this type of concrete could not increase the removal of phenol (Ph) and ammonium (NH_4) and also reduced the removal percentage of FC and P. Furthermore, PC containing Fe_2O_3 nanoparticles coated with surfactant (ENPFe-surf) increased phosphate removal in comparison with normal PC.

4. Compared to normal PC, nanoparticles in modified PC significantly affected the compressive strength and permeability. Fe_2O_3, Fe, TiO_2, ENPFe-surf and SiO_2 nanoparticles generally increased the compressive strength of the PC, whereas the permeability of such concrete could be reduced by the incorporation of these nanomaterials; as an exception, ENPFe-surf increased the rate of permeability.

Looking ahead, many emerging research areas can be found that may help to enhance the environmental benefits of PC improved with nanoparticles. Firstly, further research on mix design optimization is needed to reconcile environmental and safety concerns with mechanical and hydraulic needs, which are frequently in conflict. In this respect, insufficient contributions and confidence have been proposed for such systems in treatment, even though they provide safety and environmental advantages. Secondly, the advantages of using other types of nanoparticles in PC have yet to be investigated in the removal of other pollutants. Thirdly, diverse microstructure properties of enhanced PCs with varying nanomaterials are required for better characterization. Finally, the financial aspect and advantages of using this method and materials can be comprehensively investigated in comparison with the other methods that are currently adopted for the treatment of polluted stormwater runoff. As a result, further research and promotion of PC pavement characteristics as a multifunctional solution to critical environmental issues such as water contamination in metropolitan areas are required.

Rapid developments in the control of pollution and clean manufacturing technologies, and increased awareness regarding the environmental effects of behavioural activities among the society, may lead to a further increase in the differences in pollutant emissions between historical and recent data. Therefore, caution should be urged when focusing on historical data in current environmental investigations. The tendency of progressing data obsolescence may be to be continued in the future, even at faster rates. Furthermore, the continuing introductions of new products, methods and pollutants into the urban environment suggest that identifying important sources of stormwater pollution and the associated pollutants are a continuing process.

Author Contributions: Conceptualization, V.A.; methodology, V.A. and M.M.; validation, V.A., M.M., D.N., P.A., R.G. and M.S.; investigation, V.A. and M.M.; resources, V.A., M.M. and D.N.; data curation, V.A., M.M.; writing—original draft preparation, V.A. and M.M., D.N.; writing—review and editing, V.A., M.M., D.N., P.A., R.G. and M.S.; visualization, V.A. and M.M.; supervision, V.A.; project administration, V.A. and M.M. All authors have read and agreed to the published version of the manuscript.

Funding: This research received no external funding.

Institutional Review Board Statement: Not applicable.

Informed Consent Statement: Not applicable.

Data Availability Statement: Not applicable.

Acknowledgments: The authors of the present study would like to express their utmost gratitude and appreciation to Anand D. Jayakaran and Kefeng Zhang for their valuable support.

Conflicts of Interest: The authors declare no conflict of interest.

References

1. Alimohammadi, V.; Sedighi, M.; Jabbari, E. Response surface modeling and optimization of nitrate removal from aqueous solutions using magnetic multi-walled carbon nanotubes. *J. Environ. Chem. Eng.* **2016**, *4*, 4525–4535. [CrossRef]
2. Shamshiri, A.; Alimohammadi, V.; Sedighi, M.; Jabbari, E.; Mohammadi, M. Enhanced removal of phosphate and nitrate from aqueous solution using novel modified natural clinoptilolite nanoparticles: Process optimization and assessment. *Int. J. Environ. Anal. Chem.* **2020**, 1–20. [CrossRef]
3. Tan, T.H.; Mo, K.H.; Ling, T.-C.; Lai, S.H. Current development of geopolymer as alternative adsorbent for heavy metal removal. *Environ. Technol. Innov.* **2020**, *18*, 100684. [CrossRef]
4. Alimohammadi, V.; Sedighi, M. Reduction of TDS in Water by Using Magnetic Multiwalled Carbon Nanotubes and Optimizing with Response Surface Methodology. *J. Environ. Eng.* **2018**, *144*, 04017114. [CrossRef]

5. Alimohammadi, V.; Sedighi, M.; Jabbari, E.; Nasrollahzadeh, M. Phosphate removal from aqueous solutions using magnetic multi-walled carbon nanotube; optimization by response surface methodology. *Desalination Water Treat.* **2017**, *82*, 271–281. [CrossRef]
6. Alimohammadi, V.; Sedighi, M.; Jabbari, E. Optimization of sulfate removal from wastewater using magnetic multi-walled carbon nanotubes by response surface methodology. *Water Sci. Technol.* **2017**, *76*, 2593–2602. [CrossRef] [PubMed]
7. Alimohammadi, V.; Sedighi, M.; Jabbari, E. Experimental study on efficient removal of total iron from wastewater using magnetic-modified multi-walled carbon nanotubes. *Ecol. Eng.* **2017**, *102*, 90–97. [CrossRef]
8. Li, X.; Wei, W.; Qin, H.; Hu, Y.H. Co-effects of graphene oxide sheets and single wall carbon nanotubes on mechanical properties of cement. *J. Phys. Chem. Solids* **2015**, *85*, 39–43. [CrossRef]
9. Wang, J.; Iwasaki, R.; Bayen, A.M.; Harvey, J. Future road transportation technology. *Int. J. Transp. Sci. Technol.* **2016**, *5*, iii–iv. [CrossRef]
10. Zhang, K.; Bach, P.M.; Mathios, J.; Dotto, C.B.; Deletic, A. Quantifying the benefits of stormwater harvesting for pollution mitigation. *Water Res.* **2020**, *171*, 115395. [CrossRef]
11. Liang, X.; Cui, S.; Li, H.; Abdelhady, A.; Wang, H.; Zhou, H. Removal effect on stormwater runoff pollution of porous concrete treated with nanometer titanium dioxide. *Transp. Res. Part D Transp. Environ.* **2019**, *73*, 34–45. [CrossRef]
12. Murugan, M. Performance of Concrete Based Water Filtration System: Influence of Reduced Graphene Oxide And Accelerated Carbonation. Doctor of Philosophy Dissertation, Indian Institute of Technology Madras, University in Chennai, Chennai, India, 2017.
13. El-Sabban, H.; Eid, M.; Moustafa, Y.; Abdel-Mottaleb, M. Pomegranate peel extract in situ assisted phytosynthesis of Silver Nanoparticles decorated Reduced Graphene Oxide as superior sorbents for Zn(II) and Lead(II). *Egypt. J. Aquat. Biol. Fish.* **2020**, *24*, 525–539. [CrossRef]
14. Song, S.; Wang, H.; Song, A.; Hao, J. Superhydrogels of Nanotubes Capable of Capturing Heavy-Metal Ions. *Chem. Asian J.* **2013**, *9*, 245–252. [CrossRef]
15. Fletcher, T.D.; Shuster, W.; Hunt, W.F.; Ashley, R.; Butler, D.; Arthur, S.; Trowsdale, S.; Barraud, S.; Semadeni-Davies, A.; Bertrand-Krajewski, J.-L.; et al. SUDS, LID, BMPs, WSUD and more. The evolution and application of terminology surrounding urban drainage. *Urban Water J.* **2015**, *12*, 525–542. [CrossRef]
16. Zhang, K.; Yong, F.; McCarthy, D.T.; Deletic, A. Predicting long term removal of heavy metals from porous pavements for stormwater treatment. *Water Res.* **2018**, *142*, 236–245. [CrossRef] [PubMed]
17. Weiss, P.T.; Kayhanian, M.; Gulliver, J.S.; Khazanovich, L. Permeable pavement in northern North American urban areas: Research review and knowledge gaps. *Int. J. Pavement Eng.* **2019**, *20*, 143–162. [CrossRef]
18. Dempsey, B.A.; Swisher, D.M. Evaluation of Porous Pavement and Infiltration in Centre County, PA. *World Water Environ. Resour. Congress* **2003**, 1–11. [CrossRef]
19. Legret, M.; Colandini, V. Effects of a porous pavement with reservoir structure on runoff water: Water quality and fate of heavy metals. *Water Sci. Technol.* **1999**, *39*, 111–117. [CrossRef]
20. An alternative road construction for stormwater management in cold climates. *Water Sci. Technol.* **1995**, *32*, 79–84. [CrossRef]
21. Xie, N.; Akin, M.; Shi, X. Permeable concrete pavements: A review of environmental benefits and durability. *J. Clean. Prod.* **2019**, *210*, 1605–1621. [CrossRef]
22. Asadi, I.; Shafigh, P.; Hashemi, M.; Akhiani, A.R.; Maghfouri, M.; Sajadi, B.; Mahyuddin, N.; Esfandiari, M.; Talebi, H.R.; Metselaar, H.S.C. Thermophysical properties of sustainable cement mortar containing oil palm boiler clinker (OPBC) as a fine aggregate. *Constr. Build. Mater.* **2021**, *268*, 121091. [CrossRef]
23. López-Carrasquillo, V.; Hwang, S. Comparative assessment of pervious concrete mixtures containing fly ash and nanomaterials for compressive strength, physical durability, permeability, water quality performance and production cost. *Constr. Build. Mater.* **2017**, *139*, 148–158. [CrossRef]
24. Maghfouri, M.; Shafigh, P.; Alimohammadi, V.; Doroudi, Y.; Aslam, M. Appropriate drying shrinkage prediction models for lightweight concrete containing coarse agro-waste aggregate. *J. Build. Eng.* **2020**, *29*, 101148. [CrossRef]
25. Maghfouri, M.; Shafigh, P.; Ibrahim, Z.B.; Alimohammadi, V. Quality control of lightweight aggregate concrete based on initial and final water absorption tests. In *Proceedings of the IOP Conference Series: Materials Science and Engineering, University of Malaya, Kuala Lumpur, Malaysia, 5–6 April 2017*; IOP Publishing: Kuala Lumpur, Malaysia, 2017; Volume 210, p. 12022.
26. Rahman, K.; Barua, S.; Anwar, S.; Hasan, Z.; Islam, S. Removal of Heavy Metals from Stormwater Using Porous Concrete Pavement. *J. Mod. Mater.* **2020**, *7*, 37–44. [CrossRef]
27. Hein, D.K.; Eng, P. Development of an ASCE standard for permeable interlocking concrete pavement. In Proceedings of the 2014 Conference and Exhibition of the Transportation Association of Canada, Québec, QC, Canada, 28 September–1 October 2014.
28. Yusak, M.I.M.; Jaya, R.P.; Hainin, M.R.; Ibrahim, M.H.W. An overview on the performance of nano silica materials on the properties of porous concrete pavement. *J. Adv. Sci. Res.* **2014**, 34–42.
29. Maghfouri, M. Drying Shrinkage Strain Development of Agro-Waste Oil Palm Shell Lightweight Aggregate Concrete by Using the Experimental Result, ACI and Eurocode Prediction Models. *Int. J. Integr. Eng* **2019**, *11*, 255–263. [CrossRef]
30. Bhutta, M.A.R.; Tsuruta, K.; Mirza, J. Evaluation of high-performance porous concrete properties. *Constr. Build. Mater.* **2012**, *31*, 67–73. [CrossRef]

31. Drake, J.A.P.; Bradford, A.; Marsalek, J. Review of environmental performance of permeable pavement systems: State of the knowledge. *Water Qual. Res. J.* **2013**, *48*, 203–222. [CrossRef]
32. Ortega-Villar, R.; Lizárraga-Mendiola, L.; Coronel-Olivares, C.; López, L.D.; Bigurra-Alzati, C.A.; Vázquez-Rodríguez, G.A. Effect of photocatalytic Fe_2O_3 nanoparticles on urban runoff pollutant removal by permeable concrete. *J. Environ. Manag.* **2019**, *242*, 487–495. [CrossRef]
33. Jianming, G.; Xu, G.; Lu, X. Experimental study on eco-environmental effect of porous concrete. *J. Southeast Univ.* **2008**, *38*, 794–798.
34. Turco, M.; Brunetti, G.; Palermo, S.A.; Capano, G.; Grossi, G.; Maiolo, M.; Piro, P. On the environmental benefits of a permeable pavement: Metals potential removal efficiency and Life Cycle Assessment. *Urban Water J.* **2020**, *17*, 619–627. [CrossRef]
35. Martin, W.; Sumanasooriya, M.; Kaye, N.B.; Putman, B. Design of Porous Pavements for Improved Water Quality and Reduced Runoff. *Handb. Environ. Eng.* **2018**, 425–451. [CrossRef]
36. Madkour, L.H. Ecotoxicology of Environmental Heavy Metal Ions and Free Radicals on Macromolecule Cell Organisms. In *Bioengineering Applications of Carbon Nanostructures*; Springer Science and Business Media LLC: Berlin/Heidelberg, Germany, 2020; pp. 1–46.
37. Reza, R.; Singh, G. Heavy metal contamination and its indexing approach for river water. *Int. J. Environ. Sci. Technol.* **2010**, *7*, 785–792. [CrossRef]
38. Welker, A.L.; Barbis, J.D.; Jeffers, P.A. A Side-by-Side Comparison of Pervious Concrete and Porous Asphalt1. *JAWRA J. Am. Water Resour. Assoc.* **2012**, *48*, 809–819. [CrossRef]
39. Shabalala, A.N.; Ekolu, S.O.; Diop, S.; Solomon, F. Pervious concrete reactive barrier for removal of heavy metals from acid mine drainage—Column study. *J. Hazard. Mater.* **2017**, *323*, 641–653. [CrossRef] [PubMed]
40. Haselbach, L.; Poor, C.; Tilson, J. Dissolved zinc and copper retention from stormwater runoff in ordinary portland cement pervious concrete. *Constr. Build. Mater.* **2014**, *53*, 652–657. [CrossRef]
41. Kuang, X.; Kim, J.-Y.; Gnecco, I.; Raje, S.; Garofalo, G.; Sansalone, J.J. Particle Separation and Hydrologic Control by Cementitious Permeable Pavement. *Transp. Res. Rec. J. Transp. Res. Board* **2007**, *2025*, 111–117. [CrossRef]
42. Lee, M.-G.; Tia, M.; Chuang, S.-H.; Huang, Y.; Chiang, C.-L. Pollution and Purification Study of the Pervious Concrete Pavement Material. *J. Mater. Civ. Eng.* **2014**, *26*, 04014035. [CrossRef]
43. Solpuker, U.; Sheets, J.; Kim, Y.; Schwartz, F. Leaching potential of pervious concrete and immobilization of Cu, Pb and Zn using pervious concrete. *J. Contam. Hydrol.* **2014**, *161*, 35–48. [CrossRef]
44. Huang, J.; Valeo, C.; He, J.; Chu, A. Three Types of Permeable Pavements in Cold Climates: Hydraulic and Environmental Performance. *J. Environ. Eng.* **2016**, *142*, 04016025. [CrossRef]
45. Jiang, A.; Cheng, Z.; Shen, Z.; Guo, W. QSAR study on the removal efficiency of organic pollutants in supercritical water based on degradation temperature. *Chem. Central J.* **2018**, *12*, 16. [CrossRef] [PubMed]
46. Cui, Z.; Tian, W.; Qin, H.; Wang, X.; Zhao, W. Optimal design and control of Eastman organic wastewater treatment process. *J. Clean. Prod.* **2018**, *198*, 333–350. [CrossRef]
47. Vithanage, M.; Mayakaduwa, S.; Herath, I.; Ok, Y.S.; Mohan, D. Kinetics, thermodynamics and mechanistic studies of carbofuran removal using biochars from tea waste and rice husks. *Chemosphere* **2016**, *150*, 781–789. [CrossRef]
48. Ali, I.; Asim, M.; Khan, T.A. Low cost adsorbents for the removal of organic pollutants from wastewater. *J. Environ. Manag.* **2012**, *113*, 170–183. [CrossRef]
49. Dai, Y.; Zhang, N.; Xing, C.; Cui, Q.; Sun, Q. The adsorption, regeneration and engineering applications of biochar for removal organic pollutants: A review. *Chemosphere* **2019**, *223*, 12–27. [CrossRef]
50. Brown, R.A.; Line, D.E.; Hunt, W.F. LID Treatment Train: Pervious Concrete with Subsurface Storage in Series with Bioretention and Care with Seasonal High Water Tables. *J. Environ. Eng.* **2012**, *138*, 689–697. [CrossRef]
51. Park, S.-B.; Tia, M. An experimental study on the water-purification properties of porous concrete. *Cem. Concr. Res.* **2004**, *34*, 177–184. [CrossRef]
52. Jo, M.; Soto, L.; Arocho, M.; John, J.S.; Hwang, S. Optimum mix design of fly ash geopolymer paste and its use in pervious concrete for removal of fecal coliforms and phosphorus in water. *Constr. Build. Mater.* **2015**, *93*, 1097–1104. [CrossRef]
53. Hwang, V.; Masters, A.; Arocho, M.; Hwang, S. Fly ash-amended pervious concrete pavement followed by bamboo bioretention basin with Dracaena sanderiana for urban stormwater runoff control. *Constr. Build. Mater.* **2017**, *132*, 161–169. [CrossRef]
54. Karamalegos, A.M.; Barrett, M.E.; Lawler, D.F.; Malina, J.F. *Particle Size Distribution of Highway Runoff and Modification Through Stormwater Treatment*; Center for Research in Water Resources, University of Texas at Austin: Austin, TX, USA, 2005.
55. Soto-Pérez, L.; Hwang, S. Mix design and pollution control potential of pervious concrete with non-compliant waste fly ash. *J. Environ. Manag.* **2016**, *176*, 112–118. [CrossRef]
56. Monrose, J.; Tota-Maharaj, K.; Mwasha, A. Assessment of the physical characteristics and stormwater effluent quality of permeable pavement systems containing recycled materials. *Road Mater. Pavement Des.* **2019**, 1–33. [CrossRef]
57. American Water Works Association; Edzwald, J. *Water Quality & Treatmenta Handbook on Drinking Water*; McGraw-Hill Education: New York, NY, USA, 2011.
58. Chowdhury, R.K.; Sharvelle, S.E.; Beecham, S. Greywater quality changes in a permeable pavement reservoir. *Proc. Inst. Civ. Eng. Water Manag.* **2016**, *169*, 190–198. [CrossRef]

59. Tota-Maharaj, K.; Scholz, M. Efficiency of permeable pavement systems for the removal of urban runoff pollutants under varying environmental conditions. *Environ. Prog. Sustain. Energy* **2010**, *29*, 358–369. [CrossRef]
60. Pilon, B.S.; Tyner, J.S.; Yoder, D.C.; Buchanan, J.R. The Effect of Pervious Concrete on Water Quality Parameters: A Case Study. *Water* **2019**, *11*, 263. [CrossRef]
61. Boutilier, L.; Jamieson, R.; Gordon, R.; Lake, C.; Hart, W. Adsorption, sedimentation, and inactivation of E. coli within wastewater treatment wetlands. *Water Res.* **2009**, *43*, 4370–4380. [CrossRef] [PubMed]
62. Liu, L.; Hall, G.; Champagne, P. The role of algae in the removal and inactivation of pathogenic indicator organisms in wastewater stabilization pond systems. *Algal Res.* **2020**, *46*, 101777. [CrossRef]
63. Rusciano, G.M.; Obropta, C.C. Bioretention Column Study: Fecal Coliform and Total Suspended Solids Reductions. *Trans. ASABE* **2007**, *50*, 1261–1269. [CrossRef]
64. Xu, L.; Xian, F.; Chen, Y.; Miao, J.; Su, J.; Pei, S.; Gu, F.; Qian, L. Tunable nanoporosity in Sr-doped ZnO thin films by thermal annealing treatment and its effect on photocatalytic activity. *J. Optoelectron. Adv. Mater. J.* **2017**, *19*, 96–101.
65. Che, H.; Liu, C.; Hu, W.; Hu, H.; Li, J.; Dou, J.; Shi, W.; Li, C.; Dong, H. NGQD active sites as effective collectors of charge carriers for improving the photocatalytic performance of Z-scheme g-C_3N_4/Bi_2WO_6 heterojunctions. *Catal. Sci. Technol.* **2017**, *8*, 622–631. [CrossRef]
66. Bolt, J.R.; Zhuge, Y.; Bullen, F. The Impact of Photocatalytic on Degradation of Poly Aromatic Hydrocarbons through Permeable Concrete. 2014. Available online: http://eprints.usq.edu.au/id/eprint/27541 (accessed on 29 December 2014).
67. Liang, Z.; Ni, J. Improving the ammonium ion uptake onto natural zeolite by using an integrated modification process. *J. Hazard. Mater.* **2009**, *166*, 52–60. [CrossRef] [PubMed]
68. Ahmed, W.; Hamilton, K.; Toze, S.; Cook, S.; Page, D. A review on microbial contaminants in stormwater runoff and outfalls: Potential health risks and mitigation strategies. *Sci. Total Environ.* **2019**, *692*, 1304–1321. [CrossRef]
69. Azizullah, A.; Khattak, M.N.K.; Richter, P.; Häder, D.-P. Water pollution in Pakistan and its impact on public health—A review. *Environ. Int.* **2011**, *37*, 479–497. [CrossRef]
70. Leclerc, H.; Schwartzbrod, L.; Dei-Cas, E. Microbial Agents Associated with Waterborne Diseases. *Crit. Rev. Microbiol.* **2002**, *28*, 371–409. [CrossRef]
71. Ali, M.; Emch, M.; Donnay, J.; Yunus, M.; Sack, R. Identifying environmental risk factors for endemic cholera: A raster GIS approach. *Health Place* **2002**, *8*, 201–210. [CrossRef]
72. Nelson, E.J.; Harris, J.B.; Morris, J.G., Jr.; Calderwood, S.B.; Camilli, A. Cholera transmission: The host, pathogen and bacteriophage dynamic. *Nat. Rev. Genet.* **2009**, *7*, 693–702. [CrossRef]
73. Dewan, A.; Corner, R.; Hashizume, M.; Ongee, E.T. Typhoid Fever and Its Association with Environmental Factors in the Dhaka Metropolitan Area of Bangladesh: A Spatial and Time-Series Approach. *PLoS Negl. Trop. Dis.* **2013**, *7*, e1998. [CrossRef]
74. A Crump, J. Progress in Typhoid Fever Epidemiology. *Clin. Infect. Dis.* **2019**, *68*, S4–S9. [CrossRef]
75. Heymann, D.L. *Control of Communicable Diseases Manual*; American Public Health Association: Washington, DC, USA, 2008.
76. Ryu, S.; A Won, S.; Uh, J.; Song, J.Y. Hepatitis A Virus Infection from a Contaminated Tap of Ground Water Facility in a Neighborhood Park, Republic of Korea. *Infect. Chemother.* **2019**, *51*, 62–66. [CrossRef]
77. Hooshyar, H.; Rostamkhani, P.; Arbabi, M.; Delavari, M. Giardia lamblia infection: Review of current diagnostic strategies. *Gastroenterol. Hepatol. Bed Bench* **2019**, *12*, 3–12.
78. Gerace, E.; Presti, V.D.M.L.; Biondo, C. Cryptosporidium infection: Epidemiology, pathogenesis, and differential diagnosis. *Eur. J. Microbiol. Immunol.* **2019**, *9*, 119–123. [CrossRef]
79. Acrylamide, O. National Primary Drinking Water Regulations. *Kidney* **2009**, *2*, 7.
80. Haq, M. Surface and ground water contamination in NWFP and Sindh provinces with respect to trace elements. *Int J. Agric. Biol.* **2005**, *7*, 214–217.
81. Santos, D.; Vieira, R.; Luzio, A.; Félix, L. Zebrafish Early Life Stages for Toxicological Screening: Insights From Molecular and Biochemical Markers. *Adv. Mol. Toxicol.* **2018**, *12*, 151–179. [CrossRef]
82. Vhahangwele, M.; Khathutshelo, L. Environmental contamination by heavy metals. *Heavy Met.* **2018**, *10*, 115–132.
83. Engwa, G.A.; Ferdinand, P.U.; Nwalo, F.N.; Unachukwu, M.N. Mechanism and Health Effects of Heavy Metal Toxicity in Humans. In *Poisoning in the Modern World-New Tricks for an Old Dog*; IntechOpen: London, UK, 2019; pp. 77–100. [CrossRef]
84. Wani, A.L.; Ara, A.; Usmani, J.A. Lead toxicity: A review. *Interdiscip. Toxicol.* **2015**, *8*, 55–64. [CrossRef]
85. Prashanth, T.; Anura, K. Summary on Adverse Effects of Excess Iron. *Indian J. Community Health* **2018**, *30*, 103–107. Available online: https://www.iapsmupuk.org/journal/index.php/IJCH/article/view/822 (accessed on 1 July 2018).
86. Island, P.E.; Scotia, N.; Territories, N. *Manganese in Drinking Water*; Federal-Provincial-Territorial Committee on Drinking Water; Government of Canada: Ottawa, ON, Canada, 2016.
87. Röllin, H.; Nogueira, C. Manganese: Environmental Pollution and Health Effects. *Encycl. Environ. Health* **2011**, 617–629.
88. Idrees, N.; Tabassum, B.; Abd_Allah, E.; Hashem, A.; Sarah, R.; Hashim, M. Groundwater contamination with cadmium concentrations in some West U.P. Regions, India. *Saudi J. Biol. Sci.* **2018**, *25*, 1365–1368. [CrossRef] [PubMed]
89. Burke, F.; Hamza, S.; Naseem, S.; Nawaz-Ul-Huda, S.; Azam, M.; Khan, I. Impact of Cadmium Polluted Groundwater on Human Health. *SAGE Open* **2016**, *6*, 2158244016634409. [CrossRef]
90. Tsang, D.C.; Yu, I.K.; Xiong, X. Novel Application of Biochar in Stormwater Harvesting. *Biochar Biomass Waste* **2019**, 319–347. [CrossRef]

91. Chowdhury, S.; Khan, N.; Kim, G.-H.; Harris, J.; Longhurst, P.; Bolan, N.S. Zeolite for Nutrient Stripping From Farm Effluents. In *Environmental Materials and Waste*; Elsevier BV: Amsterdam, The Netherlands, 2016; pp. 569–589.
92. Xue, Y.; Song, J.; Zhang, Y.; Kong, F.; Wen, M.; Zhang, G. Nitrate Pollution and Preliminary Source Identification of Surface Water in a Semi-Arid River Basin, Using Isotopic and Hydrochemical Approaches. *Water* **2016**, *8*, 328. [CrossRef]
93. Parvizishad, M.; Dalvand, A.; Mahvi, A.H.; Goodarzi, F. A Review of Adverse Effects and Benefits of Nitrate and Nitrite in Drinking Water and Food on Human Health. *Health Scope* **2017**, in press. [CrossRef]
94. Singh, A.L. Nitrate and phosphate contamination in water and possible remedial measures. *Environ. Problems Plant.* **2016**, *3*, 44–56.
95. Calvo, M.S.; Uribarri, J. Public health impact of dietary phosphorus excess on bone and cardiovascular health in the general population. *Am. J. Clin. Nutr.* **2013**, *98*, 6–15. [CrossRef] [PubMed]
96. Abdel-Shafy, H.I.; Mansour, M. A review on polycyclic aromatic hydrocarbons: Source, environmental impact, effect on human health and remediation. *Egypt. J. Pet.* **2016**, *25*, 107–123. [CrossRef]
97. Marc, R. Asian textile dye makers are a growing power in changing market, C EN Northeast. *News Bureau* **1996**, *73*, 10–12.
98. Fayazi, M.; Taher, M.A.; Afzali, D.; Mostafavi, A. Enhanced Fenton-like degradation of methylene blue by magnetically activated carbon/hydrogen peroxide with hydroxylamine as Fenton enhancer. *J. Mol. Liq.* **2016**, *216*, 781–787. [CrossRef]
99. Khataeeabc, A.R.; Kasiri, M.B. Photocatalytic degradation of organic dyes in the presence of nanostructured titanium dioxide: Influence of the chemical structure of dyes. *J. Mol. Catal. A Chem.* **2010**, *328*, 8–26. [CrossRef]
100. Monib, S.; Mohamed, A.; I Abdelaziz, M. Methylene Blue Spray for Identification of Parathyroid Glands During Thyroidectomy. *Cureus* **2020**, *12*. [CrossRef]
101. Hassanpour, M.; Safardoust-Hojaghan, H.; Salavati-Niasari, M. Degradation of methylene blue and Rhodamine B as water pollutants via green synthesized Co_3O_4/ZnO nanocomposite. *J. Mol. Liq.* **2017**, *229*, 293–299. [CrossRef]
102. Waller, R.M. Ground water and the rural homeowner. *Gen. Interest Publ.* **1988**. [CrossRef]
103. Taylor, A.A.; Tsuji, J.S.; Garry, M.R.; McArdle, M.E.; Goodfellow, W.L.; Adams, W.J.; Menzie, C.A. Critical Review of Exposure and Effects: Implications for Setting Regulatory Health Criteria for Ingested Copper. *Environ. Manag.* **2020**, *65*, 131–159. [CrossRef]
104. Ayotte, J.D.; Medalie, L.; Qi, S.L.; Backer, L.C.; Nolan, B. Estimating the High-Arsenic Domestic-Well Population in the Conterminous United States. *Environ. Sci. Technol.* **2017**, *51*, 12443–12454. [CrossRef]
105. Hong, Y.-S.; Song, K.-H.; Chung, J.-Y. Health Effects of Chronic Arsenic Exposure. *J. Prev. Med. Public Health* **2014**, *47*, 245–252. [CrossRef]
106. Basu, H.; Saha, S.; Mahadevan, I.A.; Pimple, M.V.; Singhal, R.K. Humic acid coated cellulose derived from rice husk: A novel biosorbent for the removal of Ni and Cr. *J. Water Process. Eng.* **2019**, *32*, 100892. [CrossRef]
107. Genchi, G.; Carocci, A.; Lauria, G.; Sinicropi, M.S.; Catalano, A. Nickel: Human Health and Environmental Toxicology. *Int. J. Environ. Res. Public Health* **2020**, *17*, 679. [CrossRef]
108. Deda, A.; Alushllari, M.; Mico, S. *Measurement of Heavy Metal Concentrations in Groundwater*; AIP Publishing: Birmingham, UK, 2017.
109. Musa, O.K.; Shaibu, M.M.; Kudamnya, E.A. Heavy metal concentration in groundwater around Obajana and its environs, Kogi State, North Central Nigeria. *Am. Int J. Contemp Res.* **2013**, *3*, 170–177.
110. Maghfouri, M.; Shafigh, P.; Aslam, M. Optimum oil palm shell content as coarse aggregate in concrete based on me-chanical and durability properties. *Adv. Mater. Sci. Eng.* **2018**, *2018*. [CrossRef]
111. National Ready Mixed Concrete Association. *Freeze-Thaw Resistance Of Pervious Concrete*; National Ready Mixed Concrete Association: Silver Spring, MD, USA, 2004.
112. ACI Committee 522. *Report on Pervious Concrete*; American Concrete Institute: Indianapolis, IN, USA, 2010.
113. C/CM-14a. *Standard Test Method for Density and Void Content of Freshly Mixed Pervious Concrete*; ASTM International West: Conshohocken, PA, USA, 2014.
114. Neithalath, N.; Weiss, W.; Olek, J. Characterizing Enhanced Porosity Concrete using electrical impedance to predict acoustic and hydraulic performance. *Cem. Concr. Res.* **2006**, *36*, 2074–2085. [CrossRef]
115. Muñoz, A.M. *Evaluation of Sustainability, Durability and the Effect of Specimen Type in Pervious Concrete Mixtures*; Texas State University-San Marcos: San Marcos, TX, USA, 2012.
116. Matsuo, Y.; Morino, K.; Iwatsuki, E. A study of porous concrete using electric arc furnace oxidizing slag aggregate. *Bull. Aichi Inst. Technol. Part. B* **2005**, *40*, 167–217.
117. Aoki, Y. Development of Pervious Concrete. Master's Thesis, Technical University of Sydney, Sydney, Australia, 2009.
118. Lee, M.J.; Huang, Y.; Chiang, C.L. Purification Study of Pervious Concrete Pavement. *Int. J. Eng. Technol.* **2013**, *5*, 532–535. [CrossRef]
119. Malhotra, V.M. No-fines concrete-its properties and applications. *J. Proc.* **1974**, *17*, 628–644. [CrossRef]
120. Ghafoori, N.; Dutta, S. Building and Nonpavement Applications of No-Fines Concrete. *J. Mater. Civ. Eng.* **1995**, *7*, 286–289. [CrossRef]
121. Barnhouse, P.W.; Srubar, W.V. Material characterization and hydraulic conductivity modeling of macroporous recycled-aggregate pervious concrete. *Constr. Build. Mater.* **2016**, *110*, 89–97. [CrossRef]
122. Kim, G.; Jang, J.; Khalid, H.R.; Lee, H. Water purification characteristics of pervious concrete fabricated with CSA cement and bottom ash aggregates. *Constr. Build. Mater.* **2017**, *136*, 1–8. [CrossRef]

123. Luck, J.D.; Workman, S.R.; Coyne, M.S.; Higgins, S.F. Solid material retention and nutrient reduction properties of pervious concrete mixtures. *Biosyst. Eng.* **2008**, *100*, 401–408. [CrossRef]
124. Sheth, P.D.K.; Patel, M. Pervious Concrete As Environmentally Friendly Material-A review. *Int. J. Eng. Sci.* **2015**, *1*, 1–6.
125. Fu, T.C.; Yeih, W.; Chang, J.J.; Huang, R. The Influence of Aggregate Size and Binder Material on the Properties of Pervious Concrete. *Adv. Mater. Sci. Eng.* **2014**, *2014*, 1–17. [CrossRef]
126. Sata, V.; Wongsa, A.; Chindaprasirt, P. Properties of pervious geopolymer concrete using recycled aggregates. *Constr. Build. Mater.* **2013**, *42*, 33–39. [CrossRef]
127. Sun, Z.; Lin, X.; Vollpracht, A. Pervious concrete made of alkali activated slag and geopolymers. *Constr. Build. Mater.* **2018**, *189*, 797–803. [CrossRef]
128. Marolf, A.; Neithalath, N.; Sell, E.; Wegner, K.; Weiss, J.; Olek, J. Influence of Aggregate Size and Gradation on Acoustic Absorption of Enhanced Porosity Concrete. *ACI Mater. J. Am. Concr. Inst.* **2004**, *101*, 82–91.
129. Deo, O.; Sumanasooriya, M.; Neithalath, N. Permeability Reduction in Pervious Concretes due to Clogging: Experiments and Modeling. *J. Mater. Civ. Eng.* **2010**, *22*, 741–751. [CrossRef]
130. Dierkes, C.; Benze, W.; Wells., J. Sustainable urban drainage and pollutant source control by infiltration. In Proceedings of the 6th Regional Conference on Urban Stormwater, Stormwater Industry Association, Orange, Australia,, 22–26 April 2002.
131. Kevern, J.T.; Wang, K.; Schaefer, V.R. Effect of Coarse Aggregate on the Freeze-Thaw Durability of Pervious Concrete. *J. Mater. Civ. Eng.* **2010**, *22*, 469–475. [CrossRef]
132. Maghfouri, M.; Alimohammadi, V.; Azarsa, P.; Asadi, I.; Doroudi, Y.; Balakrishnan, B. Impact of Fly Ash on Time-Dependent Properties of Agro-Waste Lightweight Aggregate Concrete. *J. Compos. Sci.* **2021**, *5*, 156. [CrossRef]
133. Wan, D.S.L.Y.; Aslani, F.; Ma, G. Lightweight Self-Compacting Concrete Incorporating Perlite, Scoria, and Polystyrene Aggregates. *J. Mater. Civ. Eng.* **2018**, *30*, 04018178. [CrossRef]
134. Harker, K.T.; Mahar, J. *Use of Porous Concrete and Scoria Bases to Clean Groundwater Recharge*; Missouri University of Science and Technology: Rolla, MI, USA, 2003; Paper 41; Available online: http://scholarsmine.mst.edu/icchge/7icchge/session_06/41 (accessed on 1 July 2021).
135. Reddy, K.R.; Anderson, S.; Beena, K.S.; Burken, J.; Gingery, J.R.; Kolev, C.; Rosyidi, S.A.P.; Yano, Y. *General Report-Session 6*; Missouri University of Science and Technology: Rolla, MI, USA, 2013.
136. Holmes, R.R.; Hart, M.L.; Kevern, J.T. Heavy metal removal capacity of individual components of permeable reactive concrete. *J. Contam. Hydrol.* **2017**, *196*, 52–61. [CrossRef] [PubMed]
137. Rochmah, N.; Sarya, G.; Setiawan, F. The Use of The Semanding Tuban Limestone as A Partial Replacement of Coarse Aggregate in Concrete Mixes. In Proceedings of the 1st Asian Conference on Humanities, Industry, and Technology for Society, ACHITS 2019, Surabaya Indonesia, 30–31 July 2019.
138. Vázquez-Rivera, N.I.; Soto-Pérez, L.; John, J.N.S.; Molina-Bas, O.I.; Hwang, S.S. Optimization of pervious concrete containing fly ash and iron oxide nanoparticles and its application for phosphorus removal. *Constr. Build. Mater.* **2015**, *93*, 22–28. [CrossRef]
139. Sandoval, G.F.B.; Reyes, I.G.; Schwantes-Cezario, N.; Moura, A.C.; Toralles, B.M. Correlation between Permeability and Porosity for Pervious Concrete (PC). *DYNA* **2019**, *86*, 151–159. [CrossRef]
140. Wang, S.; Zhang, G.; Wang, B.; Wu, M. Mechanical strengths and durability properties of pervious concretes with blended steel slag and natural aggregate. *J. Clean. Prod.* **2020**, *271*, 122590. [CrossRef]
141. Islam, A.B.M.S.; Al-Kutti, W.; Alsaidan, M.; Alharbi, F.; Nasir, M.; Anwar, F. Potential of volcanic waste Scoria as an eco-friendly aggregate to produce Lightweight Concrete. *Smart Cities Symp.* **2018**, 28. [CrossRef]
142. Thomas, C.; Setién, J.; Polanco, J. Structural recycled aggregate concrete made with precast wastes. *Constr. Build. Mater.* **2016**, *114*, 536–546. [CrossRef]
143. Ozbakkaloglu, T.; Gu, L.; Gholampour, A. Short-Term Mechanical Properties of Concrete Containing Recycled Polypropylene Coarse Aggregates under Ambient and Elevated Temperature. *J. Mater. Civ. Eng.* **2017**, *29*, 04017191. [CrossRef]
144. Moore, J.G. Density of basalt core from Hilo drill hole, Hawaii. *J. Volcanol. Geotherm. Res.* **2001**, *112*, 221–230. [CrossRef]
145. Hydzik-Wiśniewska, J.; Wilk, A.; Bednarek, Ł.; Olesiak, S. Mixture of Crushed- Stone Aggregate as Material For Substructure Layers. *Stud. Geotech. Mech.* **2018**, *40*, 154–162. [CrossRef]
146. American Association of State Highway; Transportations Officials. *AASHTO Guide for Design of Pavement Structures*; The American Association of State Highway and Transportation Officials: Washington, DC, USA, 1993.
147. Chen, X.; Niu, Z.; Zhang, H.; Guo, Y.; Liu, M.; Zhou, M. Study on the metakaolin-based geopolymer pervious concrete (MKGPC) and its removal capability of heavy metal ions. *Int. J. Pavement Eng.* **2019**, 1–12. [CrossRef]
148. Weiss, P.T.; Kayhanian, M.; Khazanovich, L.; Gulliver, J.S. *Permeable Pavements in Cold Climates: State of The Art And Cold Climate Case Studies*; Center for Transportation Studies, University of Minnesota: Minneapolis, MN, USA, 2015.
149. Ramadhansyah, P.; Ibrahim, M.H.W.; Rosli, H.M.; Warid, M.N.M.; Hainin, M.R. Porous Concrete Pavement Containing Nano-Silica: Pre-Review. *Adv. Mater. Res.* **2014**, *911*, 454–458. [CrossRef]
150. Mehrabi, P.; Shariati, M.; Kabirifar, K.; Jarrah, M.; Rasekh, H.; Trung, N.T.; Shariati, A.; Jahandari, S. Effect of pumice powder and nano-clay on the strength and permeability of fiber-reinforced pervious concrete incorporating recycled concrete aggregate. *Constr. Build. Mater.* **2021**, *287*, 122652. [CrossRef]
151. Salemi, N.; Behfarnia, K. Effect of nano-particles on durability of fiber-reinforced concrete pavement. *Constr. Build. Mater.* **2013**, *48*, 934–941. [CrossRef]

152. Roychand, R.; Li, J.; De Silva, S.; Saberian, M.; Law, D.; Pramanik, B.K. Development of zero cement composite for the protection of concrete sewage pipes from corrosion and fatbergs. *Resour. Conserv. Recycl.* **2021**, *164*, 105166. [CrossRef]
153. Kawashima, S.; Hou, P.; Corr, D.; Shah, S.P. Modification of cement-based materials with nanoparticles. *Cem. Concr. Compos.* **2013**, *36*, 8–15. [CrossRef]
154. Pacheco-Torgal, F.; Jalali, S. Nanotechnology: Advantages and drawbacks in the field of construction and building materials. *Constr. Build. Mater.* **2011**, *25*, 582–590. [CrossRef]
155. Sanchez, F.; Sobolev, K. Nanotechnology in concrete—A review. *Constr. Build. Mater.* **2010**, *24*, 2060–2071. [CrossRef]
156. Keshavarzian, F.; Saberian, M.; Li, J. Investigation on mechanical properties of steel fiber reinforced reactive powder concrete containing nano-SiO_2: An experimental and analytical study. *J. Build. Eng.* **2021**, *44*, 102601. [CrossRef]
157. Said, A.; Zeidan, M.; Bassuoni, M.; Tian, Y. Properties of concrete incorporating nano-silica. *Constr. Build. Mater.* **2012**, *36*, 838–844. [CrossRef]
158. Tyson, B.M.; Abu Al-Rub, R.; Yazdanbakhsh, A.; Grasley, Z.C. Carbon Nanotubes and Carbon Nanofibers for Enhancing the Mechanical Properties of Nanocomposite Cementitious Materials. *J. Mater. Civ. Eng.* **2011**, *23*, 1028–1035. [CrossRef]
159. Yazdanbakhsh, A.; Grasley, Z.; Tyson, B.; Abu Al-Rub, R. Distribution of Carbon Nanofibers and Nanotubes in Cementitious Composites. *Transp. Res. Rec. J. Transp. Res. Board* **2010**, *2142*, 89–95. [CrossRef]
160. Toghroli, A.; Mehrabi, P.; Shariati, M.; Trung, N.T.; Jahandari, S.; Rasekh, H. Evaluating the use of recycled concrete aggregate and pozzolanic additives in fiber-reinforced pervious concrete with industrial and recycled fibers. *Constr. Build. Mater.* **2020**, *252*, 118997. [CrossRef]
161. Lv, S.; Ma, Y.; Qiu, C.; Sun, T.; Liu, J.; Zhou, Q. Effect of graphene oxide nanosheets of microstructure and mechanical properties of cement composites. *Constr. Build. Mater.* **2013**, *49*, 121–127. [CrossRef]
162. Makar, J.M.; Chan, G.W. Growth of Cement Hydration Products on Single-Walled Carbon Nanotubes. *J. Am. Ceram. Soc.* **2009**, *92*, 1303–1310. [CrossRef]
163. Metaxa, Z.S.; Konsta-Gdoutos, M.S.; Shah, S.P. Carbon nanofiber cementitious composites: Effect of debulking procedure on dispersion and reinforcing efficiency. *Cem. Concr. Compos.* **2013**, *36*, 25–32. [CrossRef]
164. Chuah, S.; Pan, Z.; Sanjayan, J.; Wang, C.; Duan, W.H. Nano reinforced cement and concrete composites and new perspective from graphene oxide. *Constr. Build. Mater.* **2014**, *73*, 113–124. [CrossRef]
165. Xu, G.; Shi, X. *Environmentally Friendly Pervious Concrete for Treating Deicer-Laden Stormwater (Phase II Final Report)*; Center for Environmentally Sustainable Transportation in Cold Climates, The University of Alaska: Fairbanks, AK, USA, 2018.
166. Ayanda, O.S.; Nelana, S.M.; Naidoo, E.B. Ultrasonic degradation of aqueous phenolsulfonphthalein (PSP) in the presence of nano-Fe/H_2O_2. *Ultrason. Sonochem.* **2018**, *47*, 29–35. [CrossRef]
167. Zhao, L.; Chen, R.; Pang, L.X.; Zhang, W.; Tan, X. Study on Photo-catalytic Efficiency and Durability of Nano-TiO_2 in Permeable Concrete Pavement Structure. In Proceedings of the IOP Conference Series: Earth and Environmental Science, Beijing, China, 20–22 September 2019; Volume 371.
168. Tota-Maharaj, K.; Coleman, N. Developing Novel Photocatalytic Cementitious Permeable Pavements for Depollution of Contaminants and Impurities in Urban Cities. In Proceedings of the 10th International Conference Environmental Engineering, Vilnius, Lithuania, 27–28 April 2017.
169. AlShareedah, O.; Nassiri, S. Pervious concrete mixture optimization, physical, and mechanical properties and pavement design: A review. *J. Clean. Prod.* **2021**, *288*, 125095. [CrossRef]
170. ASTM, C. *Standard Specification For Concrete Aggregates*; American Society for Testing and Materials: Philadelphia, PA, USA, 2003.
171. Meininger, R.C. No-fines pervious concrete for paving. *Concr. Eng. Int.* **1988**, *10*, 20–27.
172. Standard, A. *C150-07. Standard Specification for Portland Cement*; ASTM International: West Conshohocken, PA, USA, 2007.
173. ASTM, E. 647: Standard test method for measurement of fatigue crack growth rates. In *Annual Book of ASTM Standards*; West ASTM International: Conshohocken, PA, USA, 2011.
174. ASTM. *Standard Test Method for Ash in Biomass*; ASTM International West: Conshohocken, PA, USA, 2001.
175. Huang, B.; Wu, H.; Shu, X.; Burdette, E.G. Laboratory evaluation of permeability and strength of polymer-modified pervious concrete. *Constr. Build. Mater.* **2010**, *24*, 818–823. [CrossRef]
176. Kayhanian, M.; Anderson, D.; Harvey, J.T.; Jones, D.; Muhunthan, B. Permeability measurement and scan imaging to assess clogging of pervious concrete pavements in parking lots. *J. Environ. Manag.* **2012**, *95*, 114–123. [CrossRef]
177. Sonebi, M.; Bassuoni, M. Investigating the effect of mixture design parameters on pervious concrete by statistical modelling. *Constr. Build. Mater.* **2013**, *38*, 147–154. [CrossRef]
178. Sumanasooriya, M.S.; Deo, O.; Neithalath, N. Particle Packing-Based Material Design Methodology for Pervious Concretes. *ACI Mater. J.* **2012**, *109*.
179. Sumanasooriya, M.S.; Neithalath, N. Stereology-and Morphology-Based Pore Structure Descriptors of Enhanced Po-rosity (Pervious) Concretes. *ACI Mater. J.* **2009**, *106*.
180. Mahboub, K.C.; Canler, J.; Rathbone, R.; Robl, T.; Davis, B. Pervious concrete: Compaction and aggregate gradation. *ACI Mater. J.* **2009**, *106*, 523.
181. Tan, L.; Wang, J.; Liu, Q.; Sun, Y.; Jing, X.; Liu, L.; Liu, J.; Song, D. The synthesis of a manganese dioxide–iron oxide–graphene magnetic nanocomposite for enhanced uranium(vi) removal. *New J. Chem.* **2014**, *39*, 868–876. [CrossRef]

182. Putman, B.J.; Neptune, A.I. Comparison of test specimen preparation techniques for pervious concrete pavements. *Constr. Build. Mater.* **2011**, *25*, 3480–3485. [CrossRef]
183. Mousavi, S.-F.; Karami, H.; Farzin, S.; Teymouri, E. Effects of adding mineral adsorbents to porous concrete for enhancing the quality performance of urban runoff systems. *World J. Eng.* **2018**, *15*, 489–497. [CrossRef]
184. Montes, F.; Haselbach, L. Measuring Hydraulic Conductivity in Pervious Concrete. *Environ. Eng. Sci.* **2006**, *23*, 960–969. [CrossRef]
185. Rezania, M.; Panahandeh, M.; Razavi, S.; Berto, F. Experimental study of the simultaneous effect of nano-silica and nano-carbon black on permeability and mechanical properties of the concrete. *Theor. Appl. Fract. Mech.* **2019**, *104*, 102391. [CrossRef]
186. Vázquez-Rivera, N.I. Statistical Optimization Of Pervious Concrete Pavement Containing Fly Ash And Engineered Iron Oxide Nanoparticles For Runoff Quality And Quantity Controls. Ph.D. Thesis, University of Puerto Rico Mayagüez Campus, Mayagüez, PR, USA, 2014.
187. Beecham, S.; Pezzaniti, D.; Kandasamy, J. Stormwater treatment using permeable pavements. In *Proceedings of the Water Management*; Thomas Telford Ltd.: London, UK, 2012; Volume 165, pp. 161–170.
188. Imran, H.; Akib, S.; Karim, M.R. Permeable pavement and stormwater management systems: A review. *Environ. Technol.* **2013**, *34*, 2649–2656. [CrossRef] [PubMed]
189. Harada, S.; Yanbe, M. Adsorption by and artificial release of zinc and lead from porous concrete for recycling of adsorbed zinc and lead and of porous concrete to reduce urban non-point heavy metal runoff. *Chemosphere* **2018**, *197*, 451–456. [CrossRef]
190. Harada, S.; Komuro, Y. Decrease of non-point zinc runoff using porous concrete. *Chemosphere* **2010**, *78*, 488–491. [CrossRef] [PubMed]
191. Kara, I.; Tunc, D.; Sayin, F.; Akar, S.T. Study on the performance of metakaolin based geopolymer for Mn(II) and Co(II) removal. *Appl. Clay Sci.* **2018**, *161*, 184–193. [CrossRef]
192. Ge, Y.; Cui, X.; Kong, Y.; Li, Z.; He, Y.; Zhou, Q. Porous geopolymeric spheres for removal of Cu(II) from aqueous solution: Synthesis and evaluation. *J. Hazard. Mater.* **2015**, *283*, 244–251. [CrossRef]
193. Kara, I.; Yilmazer, D.; Akar, S.T. Metakaolin based geopolymer as an effective adsorbent for adsorption of zinc(II) and nickel(II) ions from aqueous solutions. *Appl. Clay Sci.* **2017**, *139*, 54–63. [CrossRef]
194. Al-Harahsheh, M.S.; Al Zboon, K.; Al-Makhadmeh, L.; Hararah, M.; Mahasneh, M. Fly ash based geopolymer for heavy metal removal: A case study on copper removal. *J. Environ. Chem. Eng.* **2015**, *3*, 1669–1677. [CrossRef]
195. Neithalath, N.; Sumanasooriya, M.S.; Deo, O. Characterizing pore volume, sizes, and connectivity in pervious concretes for permeability prediction. *Mater. Charact.* **2010**, *61*, 802–813. [CrossRef]
196. Sansalone, J.; Kuang, X.; Ranieri, V. Permeable Pavement as a Hydraulic and Filtration Interface for Urban Drainage. *J. Irrig. Drain. Eng.* **2008**, *134*, 666–674. [CrossRef]
197. Chen, X.; Niu, Z.; Zhang, H.; Lu, M.; Lu, Y.; Zhou, M.; Li, B. Design of a chitosan modifying alkali-activated slag pervious concrete with the function of water purification. *Constr. Build. Mater.* **2020**, *251*, 118979. [CrossRef]
198. Selbig, W.R.; Buer, N.; Danz, M.E. Stormwater-quality performance of lined permeable pavement systems. *J. Environ. Manag.* **2019**, *251*, 109510. [CrossRef]
199. Jang, Y.-I.; Lee, B.-J.; Lee, J.-W. Strength and Water Purification Properties of Environment-Friendly Construction Material Produced with the (D)PAOs and Zeolite. *Appl. Sci.* **2019**, *9*, 972. [CrossRef]
200. Muthu, M.; Santhanam, M.; Kumar, M. Pb removal in pervious concrete filter: Effects of accelerated carbonation and hydraulic retention time. *Constr. Build. Mater.* **2018**, *174*, 224–232. [CrossRef]
201. Kandra, H.; McCarthy, D.T.; Deletic, A.; Zhang, K. Modelling the clogging of a field filtration system used for stormwater harvesting. *Environ. Sci. Water Res. Technol.* **2020**, *6*, 993–1003. [CrossRef]
202. Debnath, B.; Sarkar, P.P. Pervious concrete as an alternative pavement strategy: A state-of-the-art review. *Int. J. Pavement Eng.* **2018**, *21*, 1516–1531. [CrossRef]
203. Ferguson, B. *Porous Pavements*; CRC Press: Boca Raton, FL, USA, 2005.
204. ACI Committee 522R. Report on Pervious Concrete, American Concrete Institute Committee 522. In *Technical Committee Document*; American Concrete Institute: Farmington Hills, MI, USA, 2010.
205. Chopra, M.; Kakuturu, S.; Ballock, C.; Spence, J.; Wanielista, M. Effect of Rejuvenation Methods on the Infiltration Rates of Pervious Concrete Pavements. *J. Hydrol. Eng.* **2010**, *15*, 426–433. [CrossRef]
206. Schaefer, V.R.; Wang, K. Mix design development for pervious concrete in cold weather climates. Sponsored by Iowa Department of Transportation. Highway Division. 2006. Available online: https://www.perviouspavement.org/downloads/Iowa.pdf (accessed on 1 July 2021).
207. Tong, B. Clogging Effects of Portland Cement Pervious Concrete. Ph.D. Thesis, Iowa State University, Ames, IA, USA, 2018.
208. Li, X.; Wang, B.; Cao, Y.; Zhao, S.; Wang, H.; Feng, X.; Zhou, J.; Ma, X. Water Contaminant Elimination Based on Metal–Organic Frameworks and Perspective on Their Industrial Applications. *ACS Sustain. Chem. Eng.* **2019**, *7*, 4548–4563. [CrossRef]
209. Wang, C.; Feng, Y.; Zhao, S.; Li, B.-L. A dynamic contaminant fate model of organic compound: A case study of Nitrobenzene pollution in Songhua River, China. *Chemosphere* **2012**, *88*, 69–76. [CrossRef]
210. Järup, L. Hazards of heavy metal contamination. *Br. Med. Bull.* **2003**, *68*, 167–182. [CrossRef] [PubMed]
211. Da'Na, E. Adsorption of heavy metals on functionalized-mesoporous silica: A review. *Microporous Mesoporous Mater.* **2017**, *247*, 145–157. [CrossRef]

212. Cheng, S.Y.; Show, P.-L.; Lau, B.F.; Chang, J.-S.; Ling, T.C. New Prospects for Modified Algae in Heavy Metal Adsorption. *Trends Biotechnol.* **2019**, *37*, 1255–1268. [CrossRef] [PubMed]
213. Kumar, V.; Parihar, R.; Sharma, A.; Bakshi, P.; Sidhu, G.P.S.; Bali, A.S.; Karaouzas, I.; Bhardwaj, R.; Thukral, A.; Gyasi-Agyei, Y.; et al. Global evaluation of heavy metal content in surface water bodies: A meta-analysis using heavy metal pollution indices and multivariate statistical analyses. *Chemosphere* **2019**, *236*, 124364. [CrossRef]
214. Smith, V.; Tilman, G.; Nekola, J. Eutrophication: Impacts of excess nutrient inputs on freshwater, marine, and terrestrial ecosystems. *Environ. Pollut.* **1999**, *100*, 179–196. [CrossRef]
215. Hathaway, J.M.; Hunt, W.F.; Graves, A.K.; Bass, K.L.; Caldwell, A. Exploring fecal indicator bacteria in a constructed stormwater wetland. *Water Sci. Technol.* **2011**, *63*, 2707–2712. [CrossRef] [PubMed]
216. Vitro, K.A.; BenDor, T.K.; Jordanova, T.V.; Miles, B. A geospatial analysis of land use and stormwater management on fecal coliform contamination in North Carolina streams. *Sci. Total Environ.* **2017**, *603-604*, 709–727. [CrossRef]
217. Senzia, M.; Mashauri, D.; Mayo, A. Suitability of constructed wetlands and waste stabilisation ponds in wastewater treatment: Nitrogen transformation and removal. *Phys. Chem. Earth Parts A/B/C* **2003**, *28*, 1117–1124. [CrossRef]
218. Dodds, W.K.; Whiles, M.R. Quality and Quantity of Suspended Particles in Rivers: Continent-Scale Patterns in the United States. *Environ. Manag.* **2004**, *33*, 355–367. [CrossRef]
219. Farrell, C.; Hassard, F.; Jefferson, B.; Leziart, T.; Nocker, A.; Jarvis, P. Turbidity composition and the relationship with microbial attachment and UV inactivation efficacy. *Sci. Total Environ.* **2018**, *624*, 638–647. [CrossRef]
220. Kehoe, S.C. Effect of agitation, turbidity, aluminium foil reflectors and container volume on the inactivation efficiency of batch-process solar disinfectors. *Water Res.* **2001**, *35*, 1061–1065. [CrossRef]
221. Foo, K.Y.; Hameed, B.H. Insights into the modeling of adsorption isotherm systems. *Chem. Eng. J.* **2010**, *156*, 2–10. [CrossRef]
222. Langmuir, I. The constitution and fundamental properties of solids and liquids. Part I. Solids. *J. Am. Chem. Soc.* **1916**, *38*, 2221–2295. [CrossRef]
223. Freundlich, H. Over the adsorption in solution. *J. Phys. Chem.* **1906**, *57*, 1100–1107.
224. Fach, S.; Geiger, W. Effective pollutant retention capacity of permeable pavements for infiltrated road runoffs determined by laboratory tests. *Water Sci. Technol.* **2005**, *51*, 37–45. [CrossRef]
225. Aldea, C.-M.; Song, W.-J.; Popovics, J.S.; Shah, S.P. Extent of Healing of Cracked Normal Strength Concrete. *J. Mater. Civ. Eng.* **2000**, *12*, 92–96. [CrossRef]
226. Andersen, J. An ignition method for determination of total phosphorus in lake sediments. *Water Res.* **1976**, *10*, 329–331. [CrossRef]
227. Abbott, C.L.; Comino-Mateos, L. In-situ hydraulic performance of a permeable pavement sustainable urban drainage system. *Water Environ. J.* **2003**, *17*, 187–190. [CrossRef]
228. Qian Chun-xiang, L. Study on the kinetic model of photocatalytic reaction of nano-titanium dioxide loaded on ce-ment-based materials. *J. Saf. Environ. Eng. Sci.* **2005**, *25*, 60–64.
229. Pacheco-Torgal, F.; Miraldo, S.; Ding, Y.; Labrincha, J. Targeting HPC with the help of nanoparticles: An overview. *Constr. Build. Mater.* **2013**, *38*, 365–370. [CrossRef]
230. Heikal, M.; El Aleem, S.; Morsi, W.M. Characteristics of blended cements containing nano-silica. *HBRC J.* **2013**, *9*, 243–255. [CrossRef]
231. Yang, J.; Jiang, G. Experimental study on properties of pervious concrete pavement materials. *Cem. Concr. Res.* **2003**, *33*, 381–386. [CrossRef]
232. Senff, L.; Labrincha, J.A.; Ferreira, V.M.; Hotza, D.; Repette, W.L. Effect of nano-silica on rheology and fresh properties of cement pastes and mortars. *Constr. Build. Mater.* **2009**, *23*, 2487–2491. [CrossRef]
233. Al-Qahtani, K.M. Cadmium removal from aqueous solution by green synthesis zero valent silver nanoparticles with Benjamina leaves extract. *Egypt. J. Aquat. Res.* **2017**, *43*, 269–274. [CrossRef]
234. Wang, X.; Guo, Y.; Yang, L.; Han, M.; Zhao, J.; Cheng, X. Nanomaterials as Sorbents to Remove Heavy Metal Ions in Wastewater Treatment. *J. Environ. Anal. Toxicol.* **2012**, *2*, 154. [CrossRef]
235. Suman; Kardam, A.; Gera, M.; Jain, V. A novel reusable nanocomposite for complete removal of dyes, heavy metals and microbial load from water based on nanocellulose and silver nano-embedded pebbles. *Environ. Technol.* **2014**, *36*, 706–714. [CrossRef]
236. Rengga, W.D.P.; Chafidz, A.; Sudibandriyo, M.; Nasikin, M.; Abasaeed, A.E. Silver nano-particles deposited on bamboo-based activated carbon for removal of formaldehyde. *J. Environ. Chem. Eng.* **2017**, *5*, 1657–1665. [CrossRef]
237. Ramsey, A.J. The Evaluation of Permeable Cementitious Media for Nutrient Removal. Master's Thesis, University of Missouri-Kansas City, Kansas City, MI, USA, 2017.
238. Doudrick, K.; Monzón, O.; Mangonon, A.; Hristovski, K.; Westerhoff, P. Nitrate Reduction in Water Using Commercial Titanium Dioxide Photocatalysts (P25, P90, and Hombikat UV100). *J. Environ. Eng.* **2012**, *138*, 852–861. [CrossRef]
239. Dylla, H.L. Quantification of The Environmental Impact of Titanium Dioxide Photocatalytic Pavements For Air Pollution Remediation. Ph.D. Thesis, Louisiana State University, Baton Rouge, LA, USA, 2013.
240. Okano, K.; Uemoto, M.; Kagami, J.; Miura, K.; Aketo, T.; Toda, M.; Honda, K.; Ohtake, H. Novel technique for phosphorus recovery from aqueous solutions using amorphous calcium silicate hydrates (A-CSHs). *Water Res.* **2013**, *47*, 2251–2259. [CrossRef] [PubMed]

241. Wang, T.; Lin, J.; Chen, Z.; Megharaj, M.; Naidu, R. Green synthesized iron nanoparticles by green tea and eucalyptus leaves extracts used for removal of nitrate in aqueous solution. *J. Clean. Prod.* **2014**, *83*, 413–419. [CrossRef]
242. An, Y.-J.; Kampbell, D.H.; Breidenbach, G.P. Escherichia coli and total coliforms in water and sediments at lake marinas. *Environ. Pollut.* **2002**, *120*, 771–778. [CrossRef]